

Ruthenium Arene Derivatives with PN Hemilabile Ligands. P–C Cleavage and Phosphine to Phosphinite Transformation

Agustín Caballero,[†] Félix A. Jalón,^{*,†} Blanca R. Manzano,[†] Gustavo Espino,[‡] Mercedes Pérez-Manrique,[‡] Antonio Mucientes,[§] Francisco J. Poblete,[§] and Miguel Maestro[⊥]

Departamento de Química Inorgánica, Orgánica y Bioquímica, Facultad de Químicas, Universidad de Castilla-La Mancha, Avenida Camilo J. Cela 10, 13071 Ciudad Real, Spain, Departamento de Química, Facultad de Ciencias, Universidad de Burgos, Plaza Misael Bañuelos s/n, 09001 Burgos, Spain, Departamento de Química Física, Facultad de Químicas, Universidad de Castilla-La Mancha, Avenida Camilo J. Cela 10, 13071 Ciudad Real, Spain, and Departamento de Química Fundamental, Faculdade de Ciências, Universidade da Coruña, Campus da Zapateira, 15071 A Coruña, Spain

Received July 23, 2004

Complexes of formula $[\text{RuCl}_2(\text{arene})(\kappa^1\text{-dpim})]$ (dpim = 2-(diphenylphosphino)-1-methylimidazole) (arene = *p*-cymene, **1a**; C_6H_6 , **1b**) were prepared by the reaction of $[\text{RuCl}_2(p\text{-cymene})]_2$ or $[\text{RuCl}_2(\text{C}_6\text{H}_6)(\text{CH}_3\text{CN})]$ with dpim. Complexes **1a** and **1b** were structurally characterized by NMR spectroscopy and X-ray diffraction. The reaction of these precursors with BF_4^- salts led, in dichloromethane, to cationic complexes of formula $[\text{RuCl}(\text{arene})(\kappa^2\text{-dpim})]\text{BF}_4$ (arene = *p*-cymene, **2a**; C_6H_6 , **2b**). However, in methanol the products were unexpected phosphinite derivatives of the type $[\text{RuCl}(\text{arene})(\text{HImMe})\{\kappa^1\text{-PPh}_2(\text{OMe})\}]\text{A}$ (A = BF_4 , arene = *p*-cymene, **3a**; C_6H_6 , **3b**; A = BPh_4 , arene = *p*-cymene, **3d**) (ImMe = methylimidazole). This transformation implies the existence of an easy P–C bond cleavage and phosphine functionalization with methanol at room temperature. The precursors **1a,b** or the analogous derivative with 2-(diphenylphosphino)pyridine (PPh_2py), $[\text{RuCl}_2(p\text{-cymene})(\kappa^1\text{-PPh}_2\text{py})]$, **1c**, reacted with HBF_4 to give cationic derivatives by protonation of the imidazole or the pyridine fragment, $[\text{RuCl}_2(\text{arene})(\kappa^1\text{-PNH})]\text{BF}_4$ (PNH = dpimH, arene = *p*-cymene, **4a**; C_6H_6 , **4b**; PNH = PPh_2pyH , arene = *p*-cymene, **4c**). In these compounds the existence of an asymmetric and bifurcated hydrogen bond $\text{NH}\cdots\text{Cl}_2$ has been structurally determined (even by X-ray studies for **4a,b**). Complexes **2a** and **4a** also yield the corresponding and analogous phosphinite derivatives in the presence of methanol-*d*₄ but at a markedly slower rate. NMR and spectrophotometric studies provided information concerning the formation of the phosphinite derivatives. It was concluded that the phosphine is not functionalized if it is not coordinated and that, very probably, a methanol solvate—intermediate between **1a** and **2a**—participates in the P–C bond cleavage and allows the aforementioned transformation. Some preliminary catalytic tests involving the transfer hydrogenation of cyclohexanone and the hydrogenation of phenylacetylene have also been carried out.

Introduction

The concept of hemilability was first introduced by Rauchfuss¹ referring to the labile coordination of several ligands bearing soft and hard donor atoms. These ligands and their coordination chemistry² have received increased interest in recent years. In general, the hard donor center is weakly coordinated and allows—by decoordination—the binding of substrates that induce

unique examples of reactivity.³ In recent years special attention has been paid to the preparation and coordination of hemilabile *P,O*-donor ligands and, in particular, to phosphinoether compounds.⁴ Potential *P,N*-donor molecules, although less frequently used, have received increased attention in the past few years as hemilabile ligands.^{2,5} An important application of complexes with hemilabile ligands is in catalysis, and several different processes have been analyzed.^{5a,6} Theoretical studies concerned with this application have been performed.⁷ Arene complexes of ruthenium have been extensively studied as catalyst precursors.^{5a,8} On the other hand, the potentially hemilabile *P,N* ligand 2-(diphenylphos-

[†] Departamento de Química Inorgánica, Orgánica y Bioquímica, Universidad de Castilla-La Mancha.

[‡] Universidad de Burgos.

[§] Departamento de Química Física, Universidad de Castilla-La Mancha.

[⊥] Universidade da Coruña.

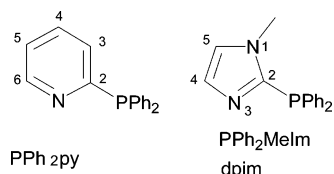
(1) Jeffrey, J. C.; Rauchfuss, T. B *Inorg. Chem.* **1979**, *18*, 2658.

(2) Braunstein, P.; Naud, F. *Angew. Chem., Int. Ed.* **2001**, *40*, 680–699.

(3) Davies, J. A.; Hartley, F. R. *Chem. Rev.* **1979**, *81*, 2658.

(4) (a) Bader, A.; Lindner, E. *Coord. Chem. Rev.* **1991**, *108*, 27. (b) Slone, C. S.; Weinggerger, D. A.; Mirkin, C. A. *Prog. Inorg. Chem.* **1999**, *48*, 233.

Chart 1



phino)-1-methylimidazole, dpim (see Chart 1), has been studied very little. This compound was first reported in 1993,⁹ although a more convenient synthetic route was subsequently published in 2001.¹⁰ Some complexes of late transition metals with the dpim ligand have been described,^{10,11} and we have reported new ruthenium derivatives containing this ligand in the three possible coordination modes: monodentate, bidentate chelate, and bridge.¹² When coordinated as a bidentate system, the relative 1,3-positions of the donor atoms in the dpim ligand are associated with a strained angle in the metallacycle after κ^2 -coordination, a situation that could favor partial decoordination of this ligand. When monocoordinated by the phosphorus atom, the ligand offers a free nitrogen that, as a basic center, could help in the activation of the substrates. With these ideas in mind, we decided to synthesize and characterize new arene ruthenium derivatives containing the dpim ligand and to undertake an initial assessment of their catalytic behavior in hydrogenation processes. It was of interest

to ascertain whether the presence of the free nitrogen atom in the case of the monocoordinated ligand could play a role similar to that of the added base in the case of transfer hydrogenation.

Interestingly, during the course of the synthesis of the new ruthenium derivatives we found an unexpected reaction of the ligand, which was transformed, by reaction with methanol, into a diarylphosphinite. These ligands are important in the field of asymmetric catalysis,¹³ and their preparation usually requires multistep and complicated procedures. A discussion concerning the role played by phosphine coordination on the Ru center and the possible mechanism of this transformation is also included. We also investigated whether this behavior was also exhibited by the similar complex containing the more frequently used ligand 2-(diphenylphosphino)pyridine^{5a,b,14} (PPh₂py) (see Chart 1).

Results and Discussion

Preparation of the New Complexes. The phosphine dpim (PN) was prepared in two steps basically in accordance with the method reported by Nishikawa,¹⁰ i.e., the reaction of *N*-methylimidazole with *n*-BuLi and reaction of the resulting salt with PCIPh₂. The ligand dpim reacts with the dimeric compounds [RuCl₂(arene)]₂ (arene = *p*-cymene, C₆H₆) to give complexes of formula [RuCl₂(arene)(κ^1 -PN)] (arene = *p*-cymene, **1a**; C₆H₆, **1b**). The poor solubility of the starting benzene derivative lowers the yield of complex **1b**, which is more conveniently prepared by the reaction of the phosphine with the monomeric adduct [RuCl₂(C₆H₆)(NCCH₃)].¹⁵ Complexes **1a** and **1b** were used as starting materials for the preparation of other new complexes according to Scheme 1.

The reactions of **1a,b** with TIBF₄ in dichloromethane gave the cationic complexes [RuCl(arene)(κ^2 -dpim)]BF₄ (arene = *p*-cymene, **2a**; C₆H₆, **2b**) by elimination of the chloride group and subsequent chelation of the phosphine. In marked contrast, a similar reaction with the addition of a solution of NaBF₄ or NaBPh₄ in methanol yielded the cationic phosphinito complexes [RuCl(arene)(MeImH)(κ^1 -PPh₂OMe)]A (A = BF₄, arene = *p*-cymene, **3a**; C₆H₆, **3b**; A = BPh₄, arene = *p*-cymene, **3d**) (MeIm = methylimidazole). These complexes can be considered the final products of a P–C(imidazolyl) bond activation and transfer of the MeIm fragment as the result of a nucleophilic attack of MeOH at the phosphorus group. Mechanistic considerations will be discussed below. The P–C bond activation by incoming nucleophiles in metal complexes has very few literature precedents,¹⁶ and it is noteworthy that, in the cases of complexes **3a**, **3b**, and **3d**, the reaction is carried out under very mild conditions. As stated above, the preparation of this type of ligand is usually a complicated process. Illustrative examples are (*S*)-BINAPO,¹⁷ glu-

(5) (a) Moldes, I.; de la Encarnación, E.; Ros, J.; Alvarez-Larena, A.; Piniella, J. F. *J. Organomet. Chem.* **1998**, *566*, 165. (b) Espinet, P.; Soulantica, K. *Coord. Chem. Rev.* **1999**, *193–195*, 499. (c) Ellermann, J.; Schelle, C.; Knoch, F. A.; Möll, M.; Pohl, D. *Monatsh. Chem.* **1996**, *127*, 783. (d) Rulke, R. E.; Kaasjager, V. E.; Wehman, P.; Elsevier, C. J.; van Leeuwen, P. W. N. M.; Vrieze, K.; Fraanje, J.; Goubitz, K.; Spek, A. L. *J. Chem. Soc., Dalton Trans.* **1996**, 3163. (e) Crociani, L.; Bandoli, G.; Dolmella, A.; Basato, M.; Corain, B. *Eur. J. Inorg. Chem.* **1998**, *11*, 1811. (f) Shen, J. Y.; Slugovc, C.; Wiede, P.; Mereiter, K.; Schmid, R.; Kirchner, K. *Inorg. Chim. Acta* **1998**, *268*, 69. (g) Hii, K. K. M.; Thornton-Pett, M.; Jutand, A.; Tooze, R. P. *Organometallics* **1999**, *18*, 1887. (h) Qadir, M.; Mochele, T.; Hii, K. K. *Tetrahedron* **2000**, *56*, 7975. (i) Pfeiffer, J.; Kickelbick, G.; Schubert, U. *Organometallics* **2000**, *19*, 62. (j) Braunstein, P.; Naud, F.; Dedieu, A.; Rohmer, M. M.; DeCian, A.; Rettig, S. J. *Organometallics* **2001**, *20*, 2966. (k) Romeo, R.; Scolaro, L. M.; Plutino, M. R.; Romeo, A.; Nicolo, F.; Del Zotto, A. *Eur. J. Inorg. Chem.* **2002**, *3*, 629.

(6) (a) Pitter, S.; Dinjus, E. *J. Mol. Catal. A: Chem.* **1997**, *125*, 39. (b) Kostas, I. D. *J. Organomet. Chem.* **2001**, *634*, 90. (c) Kostas, I. D. *J. Organomet. Chem.* **2001**, *626*, 221. (d) Kostas, I. D.; Steele, B. R.; Terzis, A.; Amosova, S. V. *Tetrahedron* **2003**, *59*, 3467. (e) Kuriyama, M.; Nagai, K.; Yamada, K.; Miwa, Y.; Taga, T.; Tomioka, K. *J. Am. Chem. Soc.* **2002**, *124*, 8932. (f) Roch-Neirey, C.; Le Bris, N.; Laurent, P.; Clement, J. C.; des Abbayes, H. *Tetrahedron Lett.* **2001**, *42*, 643. (g) Ruiz, J. L.; Flor, T.; Bayón, J. C. *Inorg. Chem. Commun.* **1999**, *2*, 484.

(7) (a) de Bruin, T. J. M.; Magna, L.; Raybaud, P.; Toulhoat, H. *Organometallics* **2003**, *22*, 3404. (b) Tobisch, S.; Ziegler, T. *Organometallics* **2003**, *22*, 5392. (c) Ramirez, A.; Lobkovsky, E.; Collum, D. B. *J. Am. Chem. Soc.* **2003**, *125*, 1537.

(8) See for example: (a) Bennett, M. A.; Huang, T.; Smith, A. K.; Turney, T. W. *J. Chem. Soc., Chem. Commun.* **1978**, 582. (b) Iwata, R.; Ogata, I. *Tetrahedron* **1973**, *29*, 2753. (c) Furstner, A.; Liebl, M.; Lehmann, C. W.; Picquet, M.; Kunz, R.; Bruneau, C.; Touchard, D.; Dixneuf, P. H. *Chem. Eur. J.* **2000**, *6*, 1847. (d) Brunner, H.; Zwack, T.; Zabel, M. *Organometallics* **2003**, *22*, 1741. (e) Nagashima, H.; Kondo, H.; Hayashida, T.; Yamaguchi, Y.; Gondo, M.; Masuda, S.; Miyazaki, K.; Matsubara, K.; Kirchner, K. *Coord. Chem. Rev.* **2003**, *245*, 177. (f) Ozdemir, I.; Cetinkaya, E.; Cetinkaya, B.; Cicek, M.; Semeril, D.; Bruneau, C.; Dixneuf, P. H. *Eur. J. Inorg. Chem.* **2004**, 418. (g) Castarlenas, R.; Fischmeister, C.; Bruneau, C.; Dixneuf, P. H. *J. Mol. Catal. A: Chem.* **2004**, *213*, 31.

(9) Tolmachev, A. A.; Yurchenko, A. A.; Semenova, M. G.; Feshchenko, N. G. *Russ. J. Chem.* **1993**, *63*, 504.

(10) Jalil, M. A.; Yamada, T.; Fujinami, S.; Honjo, T.; Nishikawa, H. *Polyhedron* **2001**, *20*, 627.

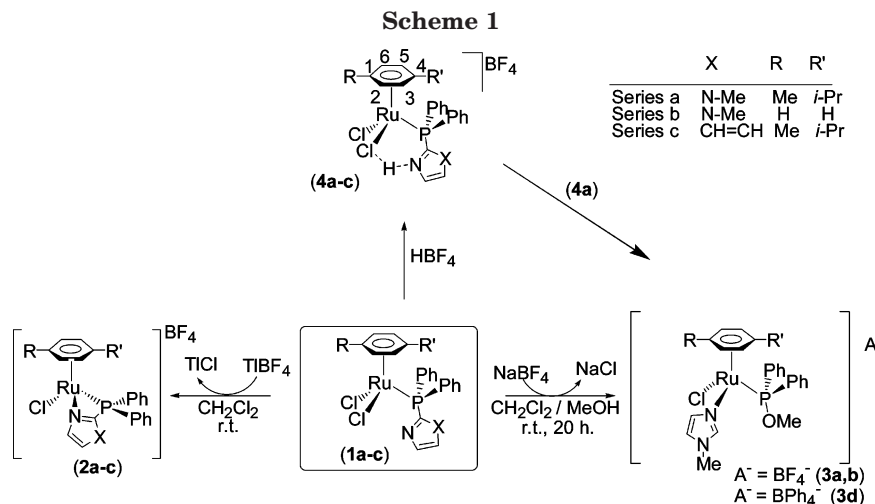
(11) Catalano, V. J.; Horner, S. J. *Inorg. Chem.* **2003**, *42*, 8430.

(12) Espino, G.; Jalón, F. A.; Maestro, M.; Manzano, B. R.; Pérez-Manrique, M.; Bacigalupe, A. C. *Eur. J. Inorg. Chem.* **2004**, 2542.

(13) Ojima, I., Ed. *Catalytic Asymmetric Synthesis*; VCH: Weinheim, Germany, 1993.

(14) (a) Newkome, G. R. *Chem. Rev.* **1993**, *93*, 2067. (b) Dervisi, A.; Edwards, P. G.; Newman, P. D.; Tooze, R. P.; Coles, S. J.; Hursthouse, M. B. *J. Chem. Soc., Dalton Trans.* **1998**, 3771. (c) Dervisi, A.; Edwards, P. G.; Newman, P. D.; Tooze, R. P. *J. Chem. Soc., Dalton Trans.* **2000**, 523. (d) Yang, H.; Gao, H.; Angelici, R. J. *Organometallics* **2000**, *19*, 622. (e) Caballero, A.; Jalón, F. A.; Manzano, B. R. *Chem. Commun.* **1998**, 1879.

(15) Takahashi, H.; Kobayashi, K.; Osawa, M. *Anal. Sci.* **2000**, *16*, 777.



cophinite,¹⁸ ProNOP,¹⁹ valNOP,²⁰ and alaNOP,²¹ or ProNOP²² derivatives. In the synthesis of these ligands the last step, where the phosphinite functional group is generated, involves the reaction of an alcohol with a phosphorus derivative under very harsh conditions.

The complex analogous to **1a** bearing *p*-cymene as the arene and PPh₂Py as the phosphine, [RuCl₂(*p*-cymene)(κ^1 -PPh₂py)] (**1c**), which has been reported previously,^{5a} was synthesized in order to analyze the possible formation of the corresponding phosphinito derivative analogous to **3a** with PPh₂py as the phosphine. However, all attempts to prepare this derivative failed and the cationic complex [RuCl(*p*-cymene)(κ^2 -PPh₂py)]BF₄, **2c**,^{5a} was the only product obtained.

Complexes with one intramolecular hydrogen bond were synthesized by the protonation of **1a–c** with HBF₄. In these reactions derivatives of formula [Ru(arene)Cl₂(κ^1 -PNH)]BF₄ (PNH = dpimH, arene = *p*-cymene, **4a**; C₆H₆, **4b**; PNH = PPh₂pyH, arene = *p*-cymene, **4c**) were obtained and characterized as complexes with NH \cdots Cl₂ hydrogen bonds (see structural discussion). It was verified that **4a**, in the presence of methanol, also evolves to **3a**, albeit at a slower rate than when **1a** is the starting material.

Structural Characterization. The FAB MS experiments (**1–3** complexes) showed molecular peaks that correspond to the loss of anions such as Cl[−] (**1a,b**), BF₄[−] (**2a,b** and **3a,b**), or BPh₄[−] (**3d**) from the mononuclear molecular mass. Peaks arising from the additional loss of the arene fragment were also observed. Complexes **3a, 3b**, and **3d** exhibited base peaks revealing the loss of methylimidazole. The easy loss of this fragment from

these complexes, but not from the rest, supports the different structural location of this group in **3a, 3b**, and **3d** (an *N*-coordinated ligand).

Structural information concerning the presence of the ligands and counteranions in the different complexes was obtained from the IR spectra (see Experimental Section).

The ³¹P NMR spectra are informative in terms of the coordination mode of the phosphine. A deshielding effect is observed in all of the complexes in the chemical shift of the dpim phosphorus signal when compared to that of the free ligand. The coordination-induced shifts (CIS) for the neutral complexes **1a,b** are relatively low. The same trend has been observed for **1c**.^{5a} This situation can be ascribed to the relative instability of the LUMO in pyramidal 16-electron two-legged piano stools.²³ This observation is also probably related with the reported stability of 16-electron [RuX₂(arene)] complexes where X₂ are π -donor ligands such as chalcogenates²⁴ or diimino groups.²⁵ A comparably low CIS is also observed for the cationic derivatives **4a–c**. The expected shielding to high field of the P resonance is observed when, in comparable complexes, the phosphine changes from the κ^1 -P to the κ^2 -PN coordination mode as a consequence of the formation of a four-membered chelate ring.²⁶

Complexes **3a, 3b**, and **3d** show ³¹P resonances at very low field, and this is a consequence of the phosphinite nature of the ligand after P–C bond activation. The chemical shifts are consistent with those observed for similar complexes.^{16c,d} Although there are exceptions, it is usually the case that the replacement of *p*-cymene by C₆H₆ induces a relative shift to low field in the P-chemical shift, probably as a consequence of the more pronounced electron-donor character of the former group.

The ¹H and ¹³C NMR spectra of these complexes are also conclusive. The resonance assignments were made on the basis of ¹H–¹H COSY, NOESY, and ¹H–¹³C COSY experiments. The *p*-cymene ligand is particularly informative with respect to the symmetry of the three-legged fragment ML₃ for complexes **1a–4a** and **4c**.

(16) Illustrative examples are: (a) Vierling, P.; Riess, J. G. *J. Am. Chem. Soc.* **1981**, *103*, 2466. (b) Van Leeuwen, P. W. N. M.; Roobeek, C. F. *Organometallics* **1990**, *9*, 2179. (c) Nakazawa, H.; Yamaguchi, Y.; Mizuta, T.; Ichimura, S.; Miyoshi, K. *Organometallics* **1995**, *14*, 4635. (d) Crochet, P.; Demerseman, B.; Rocaboy, Ch.; Scheleyer, D. *Organometallics* **1996**, *15*, 3048. (e) Yang, K.; Bott, S. G.; Richmond, M. G. *Organometallics* **1996**, *15*, 4480. (f) Geldbach, T. J.; Pregosin, P. *Eur. J. Inorg. Chem.* **2002**, 1907.

(17) Trost, B. M.; Murphy, D. J. *Organometallics* **1985**, *4*, 1143.

(18) Pino, P.; Consiglio, G. *Pure Appl. Chem.* **1983**, *55*, 1781.

(19) Mutez, S.; Mortreux, A.; Petit, F. *Tetrahedron Lett.* **1988**, *29*, 1911.

(20) Potier, Y.; Mortreux, A.; Petit, F. *J. Organomet. Chem.* **1989**, *370*, 333.

(21) Hatat, C.; Karim, A.; Kokel, N.; Mortreux, A.; Petit, F. *Tetrahedron Lett.* **1988**, *29*, 3675.

(22) Karim, A.; Mortreux, A.; Petit, F. *J. Organomet. Chem.* **1986**, *312*, 375.

(23) Hofmann, P. *Angew. Chem., Int. Ed. Engl.* **1977**, *16*, 536.

(24) Mashima, K.; Kaneko, S.; Tani, K.; Kaneyoshi, H.; Nakamura, A. *J. Organomet. Chem.* **1997**, *545–546*, 345.

(25) Haack, K.-J.; Hashiguchi, S.; Fujii, A.; Ikariya, T.; Noyori, R. *Angew. Chem., Int. Ed. Engl.* **1997**, *36*, 285.

(26) Garrow, P. E. *Chem. Rev.* **1981**, *81*, 229.

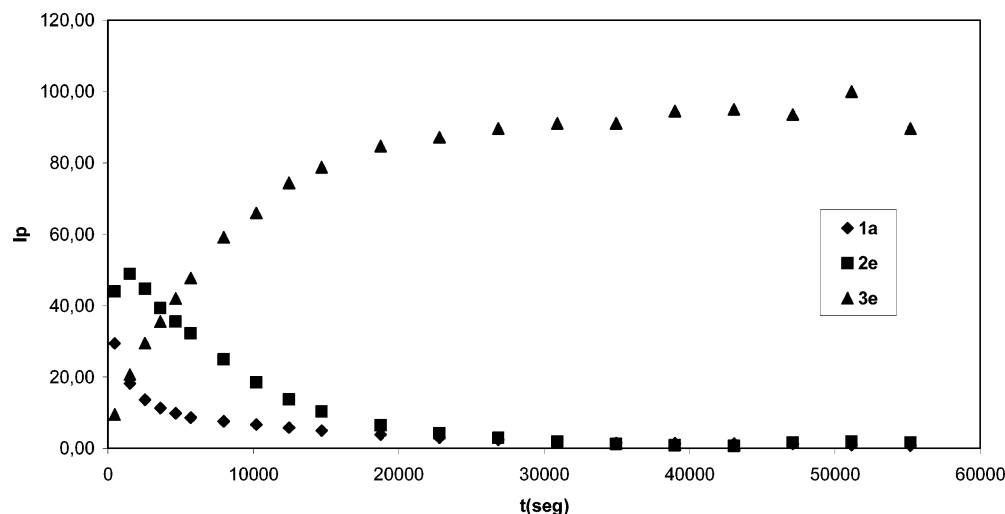


Figure 1. Plot of the transformation of **1a** to give **2e** and **3e** at 25 °C. The data were obtained from the relative intensity of the Me-Im groups in the ^1H NMR spectra. A solution of 4 mg of **1a** in a methanol- d_4 /chloroform- d ratio of 3.5 mL/1 mL was used.

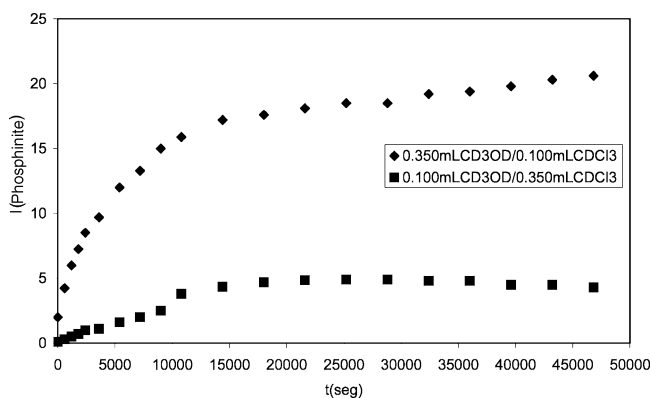


Figure 2. Plot showing the time dependence of the formation of **3e** from **1a** in deuterated solvents of different compositions at 25 °C. The data were obtained from the relative intensity of the Me-Im groups in the ^1H NMR spectra. A solution of 4 mg of **1a** was used in each experiment.

cation of **3**. Complex **2e** (the same complex as **2a** but with Cl^- as a counteranion) is formed more quickly from **1a** than **3e** (the same complex as **3a** but with Cl^- as a counteranion). The evolution of this transformation with time, starting from **1a**, is illustrated in Figure 1. (ii) The formation of **1a** from **2a** was not observed, and this is clearly a consequence of the absence of Cl^- . (iii) The formation of **3a** or **3e** is irreversible. (iv) The rate of formation of **2e** and **3e** from **1a** is enhanced when the amount of methanol- d_4 is increased in the mixture of deuterated solvents. For instance, with methanol/chloroform ratios of 3.5:1 and 1:3.5 the formation of **3e** follows the curves depicted in Figure 2. (v) The formation of **3e** or **2e** from **1a** is inhibited by the addition of chlorides (10 equiv of LiCl). (vi) When chlorides were added to the solution of **2a** (LiCl , 6.33 equiv), compounds **1a** and **2e** equilibrate in approximately 1 h. After this time **3e** is present in a very small amount in the spectra (see Figure 3). The equilibrium constant for the process $\mathbf{2e} + \text{Cl}^- \leftrightarrow \mathbf{1a}$ was found to be 11.21 mol^{-1} . (vii) An additional observation is that **1a** is not transformed into **2e** or **3e** in chloroform- d in the absence of methanol- d_4 , and (viii) the free phosphine is unaffected in pure chloroform- d or methanol- d_4 .

The mechanism depicted in Scheme 2 is reasonably consistent with all these observations. The solvate derivative **5** is included in order to account for the need for MeOH in the transformation of **1a** to **2e**. The aforementioned inhibition by chlorides on the formation of **3e** and **2e** from **1a** shows that **5** is a reasonable intermediate in the transformation of **1a** and **2e** into the phosphinite **3e**. In this way, **5** could be obtained from **1a** by methanolysis of the Ru-Cl bond. The ability of methanol to eliminate chlorides in solvolysis reactions is well documented,³¹ and the stability of **1a** in chloroform supports this proposal. The solvate intermediate **5** is shown in Scheme 2 with an $\text{OH}\cdots\text{N}$ bridge, which seems reasonable considering the ease of formation of hydrogen bonds in **4a-c**. A marked shift in the equilibrium of **1a** and **2e** with **5** toward the former compounds must exist, since **5** is not observed in any of the spectra. Consequently, it is possible to conclude that $k_{-1} > k_1$ and $k_2 > k_{-2}$. The ratio $k_1 > k_{-2}$ is deduced from the different rates of transformation of **1a** and **2b** to give **3e**.

The irreversible transformation step of **5** into **3e** can be understood in terms of an intramolecular electrophilic attack of the acid proton of the methanol onto the N^3 of the imidazole, followed by nucleophilic attack of the methanolate fragment (i1 in Scheme 3). This step, which is probably concerted, is supported by the experimental observation that **4a** is able to give the phosphinite **3a** in methanol but at a slower rate than from **1a**. The transition state proposed in Scheme 3 is reminiscent of a bridging imidazolium ion, which probably evolves to a C-coordinated carbene fragment (i2) that quickly tautomerizes to the N-coordinated imidazole group on **3e**.

The 1,2 shift and tautomerization of the imidazole fragment probably makes the P-MeIm activation irreversible. This irreversibility of the P-C cleavage induced by solvolysis has previously been observed in a few other examples.^{16d,30a}

As stated above, the chemical behavior of dpim and PPh_2py contrasts sharply as far as the P-C activation

(31) Arena, C. G.; Calamia, S.; Faraone, F.; Graiff, C.; Tiripicchio, A. *J. Chem. Soc., Dalton Trans.* **2000**, 3149.

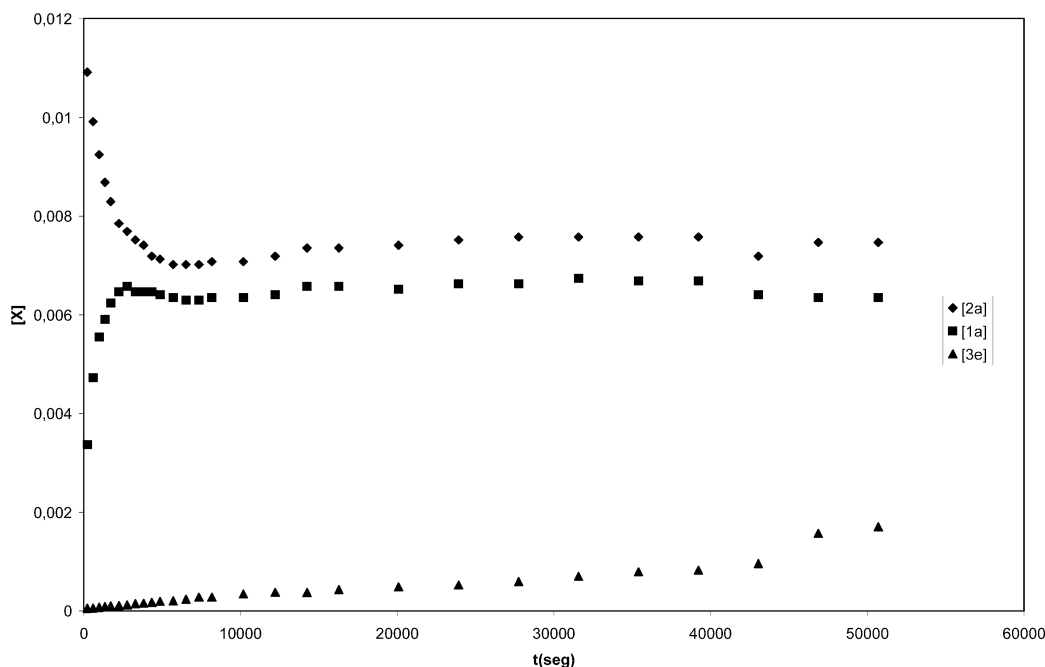
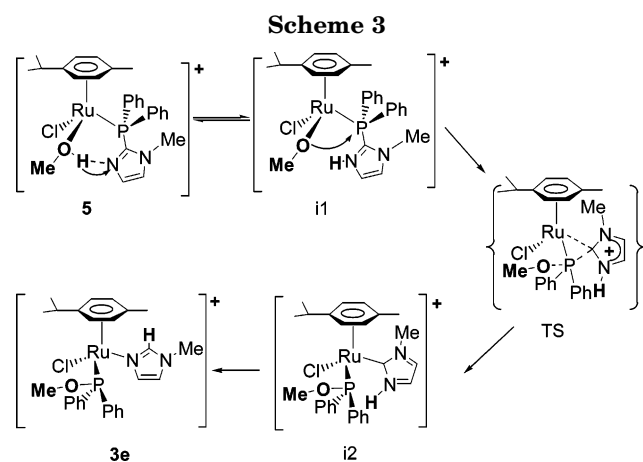


Figure 3. Plot of the transformation of **2a** into **1a** and **3e** in the presence of chlorides at 25 °C. A solution of 4 mg of **2a** and 1.6 mg of LiCl in a mixture of methanol-*d*₄/chloroform-*d* (0.350 μ L/0.100 μ L) was used.



step is concerned, probably due to the carbenic character that the imidazole group has in its quaternized state. In this carbenic form, MeImH⁺ can be considered a good leaving group and, as a consequence, the nucleophilic attack of MeO⁻ on the P atom is promoted.

To support the existence of the mechanism proposed in Scheme 2 and to extract all the possible parameters from this mechanism, a number of spectroscopic experiments were carried out. Initially, the rate constants k_1 and k_{-2} were determined spectrophotometrically by following the initial decay of **1a** and **2a** in methanol. A spectrophotometric technique was used to obtain this value due to the impossibility of following the initial decays of **1a** and **2a** in methanol using NMR techniques.

The rate constant k_1 was obtained by applying the initial rates method to the decay of **1a** in methanol, thus minimizing the importance of the reverse reaction (−1). For the decay of **1a** at 25 °C and with [MeOH] = 18.5 M, the initial rates obtained for the initial concentrations of **1a**, 6×10^{-4} and 3.5×10^{-4} M, were 4.76×10^{-7} and 2.63×10^{-7} L mol⁻¹ s⁻¹, respectively. The results show a first kinetic order with respect to **1a**. In an effort to estimate the reaction order with respect to

Table 1. Variations of the Initial Rate vs the Initial Concentration of 2a

$v_i \times 10^8$ (mol L ⁻¹ s ⁻¹)	[2a] × 10 ⁴ M			
	2.5	5	10	15
	2.52	3.78	7.86	11.3

MeOH, an initial concentration of **1a** of 3.5×10^{-4} M at 25 °C was used with MeOH concentrations of 18.5 and 12.33 M. In this case initial rates of 2.63×10^{-7} and 1.77×10^{-7} L mol⁻¹ s⁻¹ were obtained, respectively. These values also showed first order with respect to MeOH. Therefore, the disappearance rate of **1a** may be expressed as

$$-d[\mathbf{1a}]/dt = k_{\text{exp}}[\mathbf{1a}][\text{MeOH}] \quad (2)$$

The average value for the second-order rate constant k_{exp} was found to be 4.15×10^{-5} L mol⁻¹ s⁻¹. On the basis of the data obtained and the mechanism proposed in Scheme 2, this value must correspond to k_1 .

The rate constant k_{-2} was obtained by measuring the initial rates for the decay of **2a** in methanol (22.2 M) at 25 °C with different initial concentrations of this complex (see Table 1).

The plot of v_i vs [**2a**] gave a straight line ($r_{xy} = 0.998$) with a positive slope ($k_{\text{exp}}^{\text{app}} = 7.44 \times 10^{-5}$ s⁻¹) and negligible intercept; this is indicative of a first order with respect to species **2a**. A first order with respect to MeOH was also obtained. At an initial **2a** concentration of 5×10^{-4} M in methanol (22.2 and 18.5 M) at 25 °C, the respective initial rates were 3.78×10^{-8} and 3.18×10^{-8} L mol⁻¹ s⁻¹, respectively. Therefore, the experimental rate law may be expressed as follows

$$v_i = -d[\mathbf{2a}]/dt = k_{\text{exp}}[\mathbf{2a}][\text{MeOH}] \quad (3)$$

where k_{exp} was found to be 3.35×10^{-6} L mol⁻¹ s⁻¹. On the basis of the data obtained and the mechanism proposed in Scheme 2, this value must correspond to

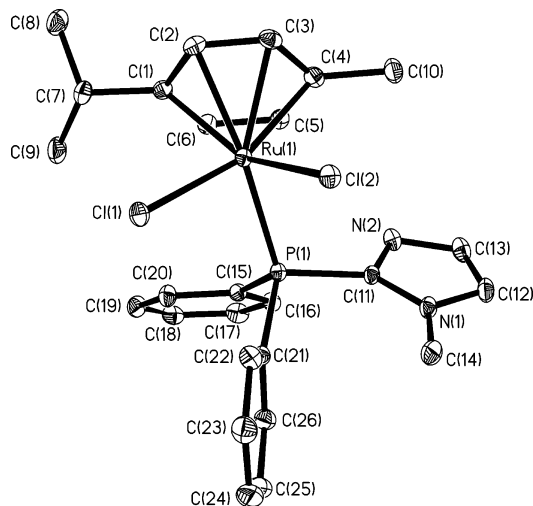


Figure 4. ORTEP view with atom numbering of complex **1a** (30% probability ellipsoids).

k_{-2} . From the decay of **2a** in the presence of chlorides (Figure 3) the concentrations of **1a** and **2a** are constant over a long time interval, and therefore, the equilibrium approximation can be used. For this interval of time the concentration of **3a** varies linearly with time. This observation is expected given the mechanism proposed (Scheme 2) and considering that the concentration of **5** must be constant when **1a** and **2a** reach the equilibrium.

$$\frac{d[3a]}{dt} = k_3[5]_e \quad (4)$$

The concentration of **5** may be calculated from the equilibria between **1a** \leftrightarrow **5** and between **2a** \leftrightarrow **5** (Scheme 2). Thus eq 4 is reduced to eq 5.

$$\frac{d[3a]}{dt} = \frac{k_3 k_1 [1a]_e [MeOH]_e}{k_{-1} [Cl^-]_e} = \frac{k_3 k_{-2} [2a]_e [MeOH]_e}{k_2} \quad (5)$$

The slope of the plot **[3a]** vs t , $d[3a]/dt$, was $1.81 \times 10^{-8} \text{ mol L}^{-1} \text{ s}^{-1}$. By inserting the values of $[1a]_e = 0.00634 \text{ M}$, $[2a]_e = 0.00707 \text{ M}$, $[MeOH]_e = 24.7 \text{ M}$, and $[Cl^-]_e = 0.0801 \text{ M}$ in eq 5 and taking into account the values of k_1 and k_{-2} above cited, the following relations were obtained: $k_{-1} = 4491k_3$, $k_2 = 32.4k_3$, and $k_{-1} = 139k_2$.

Moreover, the global equilibrium constant, corresponding to the steps (1) and (2) of the Scheme 2, can be obtained as follows.

$$K = \frac{[1a]_e}{[2a]_e [Cl^-]_e} = \frac{k_{-2} k_{-1}}{k_2 k_1} = 11.21 \text{ L mol}^{-1} \quad (6)$$

X-ray Molecular Structures of $1a \cdot 1/2CH_2Cl_2$, $1b \cdot 2CH_2Cl_2$, $4a \cdot CH_2Cl_2$, and $4b$. The molecular structures of the title complexes (see Figures 4–7) were determined by X-ray diffraction. The crystallographic data and a selection of bond distances and angles are given in Tables 2 and 3, respectively. The structures are essentially very similar as far as the molecular backbone is concerned. The arene ruthenium fragment is linked to two chlorides and a phosphine to give a three-legged piano-stool structure. In **4a,b** the dpim ligand is protonated and the BF_4^- counteranion is also present. Bond

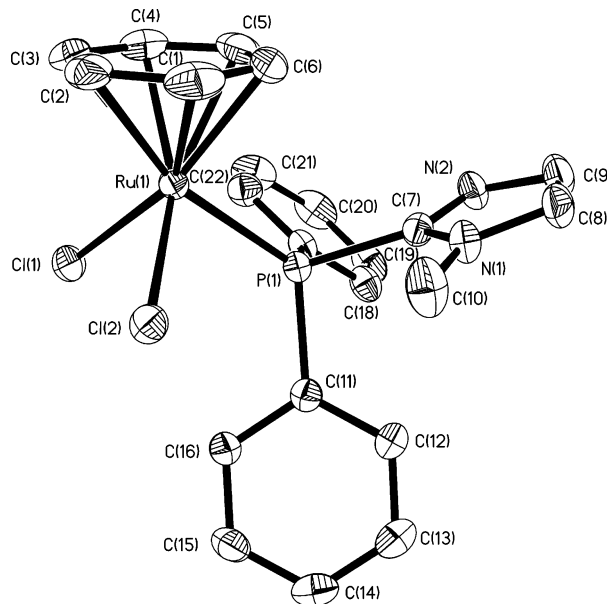


Figure 5. ORTEP view with atom numbering of complex **1b** (30% probability ellipsoids).

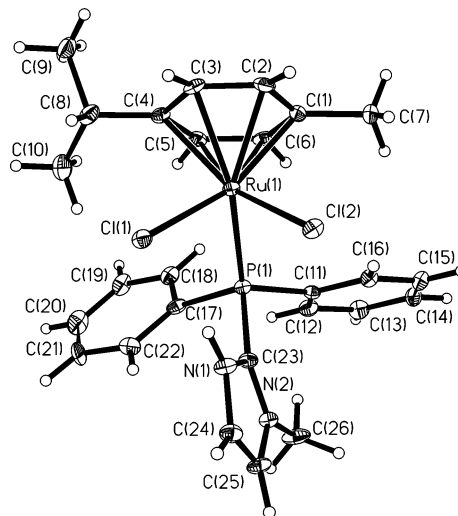


Figure 6. ORTEP view with atom numbering of the cation of complex **4a** (30% probability ellipsoids).

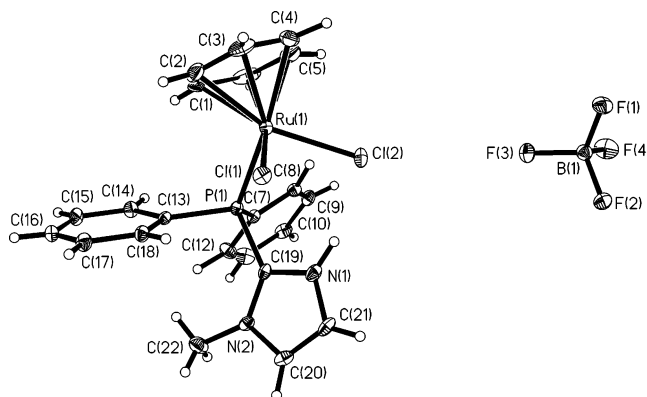


Figure 7. ORTEP view with atom numbering of complex **4b** (30% probability ellipsoids).

lengths and angles are in the range of those found in other X-ray structures of $[Ru(\text{arene})Cl_2(\text{phosphine})]$ compounds.^{5a,27,32,33} Ru–arene bond lengths are also in the range found for other arene structures. A hetero-

Table 2. Crystal Data and Structure Refinement for 1a·1/2CH₂Cl₂, 1b·2CH₂Cl₂, 4a·CH₂Cl₂, and 4b

	1a·1/2CH ₂ Cl ₂	1b·2CH ₂ Cl ₂	4a·CH ₂ Cl ₂	4b
empirical formula	C _{26.50} H ₃₀ Cl ₃ N ₂ PRu	C ₂₄ H ₂₅ Cl ₆ N ₂ PRu	C ₂₇ H ₃₂ BCl ₄ F ₄ N ₂ PRu	C ₂₂ H ₂₂ BCl ₂ F ₄ N ₂ PRu
fw	614.91	686.20	745.20	604.17
temp (K)	173(2)	298(2)	173(2)	173(2)
wavelength (Å)	0.71073	0.71073	0.71073	0.71073
cryst syst	monoclinic	monoclinic	monoclinic	monoclinic
space group	<i>P</i> 2/ <i>n</i>	<i>C</i> 2/ <i>c</i>	<i>P</i> 2(1)/ <i>n</i>	<i>P</i> 2(1)/ <i>n</i>
<i>a</i> (Å)	14.1253(9)	36.913(2)	12.661(2)	10.180(6)
<i>b</i> (Å)	10.7073(7)	36.913(2)	16.226(3)	13.035(7)
<i>c</i> (Å)	17.442(1)	24.961(1)	15.069(3)	17.884(10)
α (deg)	90	90	90	90
β (deg)	96.701(1)	127.409(1)	92.015(3)	94.892(12)
γ (deg)	90	90	90	90
volume (Å ³)	2620.0(3)	5629.2(5)	3093.9(9)	2364(2)
<i>Z</i> , calcd density (g/cm ³)	4, 1.559	8, 1.619	4, 1.600	4, 1.697
absorp coeff (cm ⁻¹)	0.0984	0.1201	0.0950	0.1002
<i>F</i> (000)	1252	2752	1504	1208
cryst size (mm)	0.50 × 0.41 × 0.10	0.35 × 0.10 × 0.10	0.32 × 0.28 × 0.15	0.16 × 0.10 × 0.10
limiting indices	-18 ≤ <i>h</i> ≤ 18, -14 ≤ <i>k</i> ≤ 14, -23 ≤ <i>l</i> ≤ 13	-31 ≤ <i>h</i> ≤ 45, -9 ≤ <i>k</i> ≤ 9, -30 ≤ <i>l</i> ≤ 28	-15 ≤ <i>h</i> ≤ 15, -20 ≤ <i>k</i> ≤ 8, -18 ≤ <i>l</i> ≤ 18	-12 ≤ <i>h</i> ≤ 12, -16 ≤ <i>k</i> ≤ 16, -22 ≤ <i>l</i> ≤ 16
no. of rflns collected/unique	17 872/6517	16 289/5527	16 306/6131	13 584/4842
<i>R</i> _{int} /restraints/params	0.0522/0/424	0.0579/0/307	0.0545/0/361	0.0657/0/386
goodness-of-fit on <i>F</i> ²	0.945	0.961	1.083	0.976
final <i>R</i> indices [<i>I</i> > 2σ(<i>I</i>)] ^a	<i>R</i> 1 = 0.0348, w <i>R</i> 2 = 0.0678	<i>R</i> 1 = 0.0407, w <i>R</i> 2 = 0.0884	<i>R</i> 1 = 0.0451, w <i>R</i> 2 = 0.1117	<i>R</i> 1 = 0.0397, w <i>R</i> 2 = 0.0648
<i>R</i> indices (all data) ^a	<i>R</i> 1 = 0.0593, w <i>R</i> 2 = 0.0753	<i>R</i> 1 = 0.0733, w <i>R</i> 2 = 0.0992	<i>R</i> 1 = 0.0845, w <i>R</i> 2 = 0.1384	<i>R</i> 1 = 0.0784, w <i>R</i> 2 = 0.0743
weights ^b (<i>a</i> , <i>b</i>)	0.0383, 0	0.0519, 0	0.0665, 0	0.0224, 0
largest diff peak and hole (e·Å ⁻³)	0.798 and -0.686	0.628 and -0.592	0.875 and -0.971	0.465 and -0.455

^a *R*1 = Σ||*F*_o| - |*F*_c||/Σ|*F*_o|; w*R*2 = [Σ[w(*F*_o² - *F*_c²)²]/Σ[w(*F*_o²)²]]^{0.5}. ^b The weighting scheme employed was *w* = [σ²(*F*_o)² + (*aP*)² + *bP*] and *P* = (|*F*_o|² + 2|*F*_c|²)³.

Table 3. Selected Bond Distances (Å) and Bond Angles (deg) of Complexes 1a·1/2CH₂Cl₂, 1b·2CH₂Cl₂, 4a·CH₂Cl₂, and 4b

	1a·1/2CH ₂ Cl ₂	1b·2CH ₂ Cl ₂	4a·CH ₂ Cl ₂	4b
Ru(1)–Cl(1)	2.4070(7)	2.4055(10)	2.3982(13)	2.3982(13)
Ru(1)–Cl(2)	2.4320(7)	2.4085(11)	2.4221(15)	2.4221(15)
Ru(1)–P(1)	2.3523(7)	2.3529(10)	2.3404(14)	2.3404(14)
Ru(1)–C(1)	2.243(3)	2.180(4)	2.159(5)	2.159(5)
Ru(1)–C(2)	2.243(3)	2.260(4)	2.174(5)	2.174(5)
Ru(1)–C(3)	2.225(3)	2.245(4)	2.219(4)	2.219(4)
Ru(1)–C(4)	2.218(3)	2.195(5)	2.220(5)	2.220(5)
Ru(1)–C(5)	2.161(3)	2.164(4)	2.175(5)	2.175(5)
Ru(1)–C(6)	2.193(3)	2.172(4)	2.177(5)	2.177(5)
Cl(1)–Ru(1)–Cl(2)	92.10(2)	87.10(4)	87.08(5)	87.08(5)
P(1)–Ru(1)–Cl(1)	87.99(2)	87.84(4)	87.70(5)	87.70(5)
P(1)–Ru(1)–Cl(2)	85.32(2)	90.13(4)	90.96(4)	90.96(4)
N(1)–Cl(2)			3.2314(4)	3.0521(16)
N(1)–Cl(1)			3.0093(5)	3.1714(12)
H(1A)–Cl(2)			2.8809(5)	2.2120(11)
H(1A)–Cl(1)			2.2843(4)	2.8571(11)
N(1)–H(1A)			0.881(1)	0.9062(5)
N(1)–H(1A)–Cl(1)			139.64(1)	101.97(3)
N(1)–H(1A)–Cl(2)			105.65(1)	153.83(5)

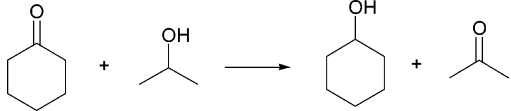
geneous distribution of the Ru–C(arene) bond distances was observed in the sense that distances *trans* to the more strongly donating phosphine group are longer than those *trans* to the chlorine atoms. This observation has been discussed elsewhere,³⁴ and it seems to be a consequence of the different donor character of the ligands in the legs of the piano stool. For the neutral complexes **1a** and **1b**, the phosphine conformation

around the Ru–P axis means that one of the phenyl groups is located in an *anti* orientation with respect to the arene moiety. In contrast, in the structure of the cations of **4a**, **b**, the MeIm group replaces the aforementioned phenyl in this position. This apparently fortuitous arrangement is very probably linked with one of the most important features of these structures, namely, the existence of a strong hydrogen bond. The bridging proton is clearly centered in the MeIm group with a short N(1)–H(1A) distance of 0.88 Å. This functional group points toward the two chlorine groups with two short H(1A)–Cl bond distances of 2.881 (Cl(2)) and 2.285 (Cl(1)) Å (**4a**) and 2.212 (Cl(2)) and 2.857 (Cl(1)) Å (**4b**). In each complex both bond lengths are shorter than the corresponding sum of van der Waals' radii, which is

(32) (a) Bennett, M. A.; Robertson, G. B.; Smith, A. K. *J. Organomet. Chem.* **1972**, *43*, C41. (b) Yamamoto, Y.; Sato, R.; Matsuo, F.; Sudoh, C.; Igoshi, T. *Inorg. Chem.* **1996**, *35*, 2329.

(33) (a) Therrier, B.; Ward, T. R.; Pilkington, M.; Hoffmann, C.; Giraltoni, F.; Weber, J. *Organometallics* **1998**, *17*, 330. (b) Therrier, B.; Ward, T. R. *Organometallics* **1999**, *18*, 1565.

(34) (a) Siedle, A. R.; Newmark, R. A.; Pignolet, L. H.; Wang, D. X.; Albright, T. A. *Organometallics* **1986**, *5*, 38. (b) Ghebreyessus, K.; Nelson, J. H. *J. Organomet. Chem.* **2003**, *669*, 48.

Table 4. Results of the Catalytic Tests for the Hydrogenation of Cyclohexanone with 2-Propanol^a


catalyst	TOF (h ⁻¹) ^b	yield (%) ^b	S:cat.	KOH/cat.
1a	182	9.1	2000:1	
1a	418	21	2000:1	333:1
2a	2.5	0.5	500:1	
2a	54	13.5	500:1	100:1

^a The reaction was carried out at reflux temperature. See Experimental Section for more details. ^b These parameters were determined after 1 h of reaction.

estimated to be 3.0 Å. This implies the existence of an asymmetric and bifurcated hydrogen bond. In this bridge, the smaller distance is very short when compared with reported hydrogen bonds involving an NH...Cl interaction in Ru or Ir complexes.³⁵ In **4a**, the Cl(1)–N(1) distance of 3.01 Å, which is shorter than the Cl(2)–N(1) bond (3.23 Å), confirms the previous statement regarding the existence of an asymmetric and bifurcated hydrogen bond. Similarly, in **4b** the two Cl–N distances are short but different. In our opinion this is a consequence of a very efficient location and orientation of the MeImH group, which favors such types of bonds.

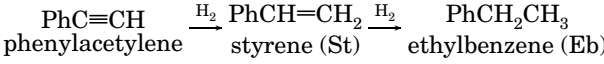
Catalytic Behavior of Compounds 1a and 2a in Hydrogenation Processes. According to the literature, arene Ru(II) complexes are good precursors for catalytic hydrogenation processes.^{5a,8a,b,25,34b,36,37} We therefore carried out preliminary tests on the catalytic activity of complexes **1a** and **2a** both in transfer hydrogenation and in hydrogenation with molecular hydrogen. These preliminary results are given in Tables 4 and 5.

First, we found that **1a** is active in the transfer hydrogenation (see Table 4) of cyclohexanone using 2-propanol as the hydrogen donor, even in the absence of an external base. The TOF is 182, which is a

(35) (a) Fryzuk, M. D.; MacNeil, P. A.; Rettig, S. J. *J. Am. Chem. Soc.* **1987**, *109*, 2803. (b) Clark, G. R.; Hodgson, D. J.; Ng, M. M. P.; Rickard, C. E. F.; Roper, W. R.; Wright, L. J. *Chem. Commun.* **1988**, 1552. (c) Fryzuk, M. D.; Montgomery, C. D.; Rettig, S. J. *Organometallics* **1991**, *10*, 467. (d) Redmore, S. M.; Rickard, C. E. F.; Webb, S.; Wright, L. J. *Inorg. Chem.* **1997**, *36*, 4743. (e) Durran, S. E.; Smith, M. B.; Slawin, A. M. Z.; Steed, J. W. J. *Chem. Soc., Dalton Trans.* **2000**, 2771. (f) Velders, A. H.; Ugozzoli, F.; Biagini-Cingi, M.; Manotti-Lanfredi, A. M.; Haasnoot, J. G.; Jan Reed, K. J. *Eur. J. Inorg. Chem.* **1999**, 213. (g) Dutta, S.; Bhattacharya, P. K.; Horn, E.; Tiekink, E. R. T. *Polyhedron* **2001**, *15–16*, 1815.

(36) (a) Rath, R. K.; Nethaji, M.; Chakravarty, A. R. *Polyhedron* **2001**, *20*, 2735. (b) Polborn, K.; Severin, K. *Chem. Eur. J.* **2000**, *6*, 4604.

(37) (a) Hashiguchi, S.; Fujii, A.; Takehara, J.; Ikariya, T.; Noyori, R. *J. Am. Chem. Soc.* **1995**, *117*, 7562. (b) Fujii, A.; Hashiguchi, S.; Uematsu, N.; Ikariya, T.; Noyori, R. *J. Am. Chem. Soc.* **1996**, *118*, 2521. (c) Matsumura, K.; Hashiguchi, S.; Ikariya, T.; Noyori, R. *J. Am. Chem. Soc.* **1997**, *119*, 8738. (d) Takehara, J.; Hashiguchi, S.; Fujii, A.; Shimichi, I.; Ikariya, T.; Noyori, R. *Chem. Commun.* **1996**, 233. (e) Noyori, R.; Hashiguchi, S. *Acc. Chem. Res.* **1997**, *30*, 97. (f) Yamakawa, M.; Ito, H.; Noyori, R. *J. Am. Chem. Soc.* **2000**, *122*, 1466. (g) Palmer, M. J.; Walsgrove, T.; Wills, M. J. *Org. Chem.* **1997**, *62*, 5226. (h) Alonso, D. A.; Brandt, P.; Nordin, S. J. M.; Andersson, P. G. *J. Am. Chem. Soc.* **1999**, *121*, 9580. (i) Petra, D. G. I.; Kamer, P. C. J.; van Leeuwen, P. W. M. N.; Goubitz, K.; Van Loon, A. M.; de Vries, J. G.; Schoemaker, H. E. *Eur. J. Inorg. Chem.* **1999**, 2335. (j) Schwink, L.; Ireland, T.; Püntener, K.; Knochel, P. *Tetrahedron: Asymmetry* **1998**, *9*, 1143. (k) Everaere, K.; Mortreux, A.; Bulliard, M.; Brussee, J.; van der Gen, A.; Nowogrocki, G.; Carpentier, J. F. *Eur. J. Org. Chem.* **2001**, 275. (l) Pastó, M.; Riera, A.; Pericàs, M. A. *Eur. J. Org. Chem.* **2002**, 2337.

Table 5. Results of the Catalytic Tests of Hydrogenation of Phenylacetylene with Molecular Hydrogen^a


catalyst	TOF (h ⁻¹) ^b [(St)/(Eb)]	yield (%) ^b [(St)/(Eb)]	conv (%) ^b	conv (%) ^c	S:cat.	solvent
1a	217/53	21.7/5.3	27	59.6	1000:1	CH ₂ Cl ₂
2a	195/141	19.5/14.1	33.6	35.0	1000:1	CH ₂ Cl ₂
2a	199/72	19.9/7.2	27.1	39.4	1000:1	<i>i</i> -PrOH

^a The reaction was carried out at 80 °C with 30 atm of H₂. See also Experimental Section. ^b These parameters were determined after 1 h of reaction. ^c Determined after 16 h of reaction.

noteworthy result if we take into account that most catalysts are inactive under these circumstances. In fact, **2a** is almost inactive in the absence of added base, since it exhibits a negligible activity (TOF = 2.5). As expected, the results are better for both precatalysts in the presence of an external base. The differences between **1a** and **2a** are probably related to the coordination mode of the phosphine. We can envisage that the free imidazolyl nitrogen in **1a** plays, in some way, the role of the base in the accepted mechanism. The bidentate coordination mode of the phosphine in **2a** prevents the imidazolyl nitrogen from playing the same role.

We also tested the catalytic activity of **1a** and **2a** in the hydrogenation of phenylacetylene with molecular hydrogen (see Table 5). These experiments were performed without the addition of base. On using both precursors, the predominant product is styrene at the beginning of the reaction, but ethylbenzene is also detected. The relative amount of ethylbenzene increases with time. This fact means that, in both cases, not only is the triple bond of the phenylacetylene hydrogenated, but also the double bond of the resulting styrene.

The cationic complex **2a** shows a better activity than **1a**, which is in agreement with the results obtained by Moldes and co-workers for the analogous arene Ru(II) complexes derived from PPh₂Py.^{5a} Apparently, in this case, the noncoordinated nitrogen does not have a positive effect. This is in accordance with a mechanism implying the homolytic activation of the molecular hydrogen. Finally, the presence of a solvent such as 2-propanol decreases the catalytic activity, as can be seen from the comparison of the results for **2a**.

We would like to emphasize that these are preliminary catalytic tests and that the reaction conditions were not optimized. Although the conversions are rather low, it is noteworthy that the substrate:catalyst ratio used in our experiments is clearly high (2000:1, 1000:1, or 500:1), especially when compared with the more common ratios used of 200, 100, or even 15 (see for example, refs 5a, 34b, 37k,l).

Conclusions

We have prepared and characterized new arene ruthenium(II) complexes containing the potentially hemilabile ligand 2-(diphenylphosphino)-1-methylimidazole (dpim). In some cases, the behavior has been compared with that of complexes containing the similar ligand, 2-(diphenylphosphino)pyridine (PPh₂py). The transformation of the neutral derivatives of the type [RuCl₂(arene)(κ¹-PN)] into the cationic species [RuCl-

(arene)(κ^2 -PN)X was achieved despite the fact that the metallacycle formed in the case of the dpim ligand would be expected to have considerable strain. Protonation of the neutral derivatives with HBF_4 led to the complexes $[\text{RuCl}_2(\text{arene})(\kappa^1\text{-PNH})]\text{BF}_4$, which exhibit a hydrogen bond. The neutral, cationic and protonated complexes containing the dpim ligand react with methanol to give the derivatives $[\text{RuCl}(\text{arene})(\text{HImMe})\{\text{PPh}_2(\text{OMe})\}]\text{BF}_4$ (Im = imidazolyl). In these complexes an unexpected activation of the phosphine ligand is observed and this implies that cleavage of the P–C(ImMe) bond has taken place. Such a process leads to the formation of a phosphinite ligand under very mild conditions. We believe that this reaction can be applied to other alcohols including commercially available chiral examples. The derivatives containing the PPh_2py ligand do not undergo this transformation. Proposals concerning the mechanism of the transformation and the different behavior of the two ligands are presented. Several derivatives have been characterized by X-ray diffraction studies, and these show a three-legged piano-stool structure. The complexes $[\text{RuCl}_2(\text{arene})(\kappa^1\text{-PNH})]\text{BF}_4$ exhibit a bifurcated and asymmetric hydrogen bond, $\text{NH}\cdots\text{Cl}_2$, in the solid state. The protonation process determines the disposition of the imidazolyl group in the dpim ligand. Preliminary catalytic tests involving hydrogenation have been performed. It is concluded that probably the pendant imidazolyl nitrogen in some way plays the role of the external base in transfer hydrogenation processes, while it does not produce a positive effect in the hydrogenation with molecular hydrogen.

Experimental Section

General Methods. All manipulations were carried out under an atmosphere of dry oxygen-free nitrogen using standard Schlenk techniques. Solvents were distilled from the appropriate drying agents and degassed before use. Elemental analyses were performed with a Perkin-Elmer 2400 CHN microanalyzer. The best analytical data were obtained for the complexes crystallized to make the X-ray structure determinations. Although in some other cases the data were totally accurate, at least in one member of each family the agreement of calculated and found values for carbon is $\pm 0.4\%$. In any case, complexes **1–4** were obtained in enough analytic purity to be used as starting materials. IR spectra were recorded on a Nicolet Impact 410 spectrophotometer as KBr pellets or on a Perkin-Elmer 883 (4000–200 cm^{-1} range) as Nujol mulls deposited on a polyethylene film. FAB mass spectra (position of the peaks in DA) were recorded with an Autospec spectrometer (University of Zaragoza). NMR spectra were recorded at room temperature ($\approx 25^\circ\text{C}$), unless stated otherwise, on a Varian Unity Inova-400 (400 MHz for ^1H ; 161.9 MHz for ^{31}P ; 100.6 MHz for ^{13}C), and a Varian UNITY-300 (300 MHz for ^1H ; 121.4 MHz for ^{31}P ; 75.4 MHz for ^{13}C) spectrometer. ^1H shifts were recorded using the residual proton of the solvent as internal standard (see numbering scheme in Chart 1). All ^{31}P shifts were referenced internally. COSY spectra: standard pulse sequence, acquisition time 0.214 s, pulse width 10 μs , relaxation delay 1 s, 16 scans, 512 increments. The NOE difference spectra were recorded with 5000 Hz, acquisition time 3.27 s, pulse width 90° , relaxation delay 4 s, and irradiation power 5–10 dB. The probe temperature (± 1 K) was controlled by a standard unit calibrated with a methanol reference. The value of k for the proton transfer in complex **4c** was calculated on the basis of the broadening in excess of the natural line width, W ($k = \pi W$). The values of the activation energy were then calculated according to the

Arrhenius theory. The gas chromatographic (GC) analyses for the reaction products of the catalytic reactions were performed on a Hewlett-Packard 5890 with a flame ionization detector chromatograph. Starting materials: $[\text{RuCl}_2(p\text{-cymene})]_2$,³⁸ $[\text{RuCl}_2(\text{C}_6\text{H}_6)]_2$,³⁸ $[\text{RuCl}(\text{C}_6\text{H}_6)(\text{CH}_3\text{CN})]$,¹⁵ and dpim¹⁰ were prepared according to literature procedures. TIBF_4 , NaBF_4 , and HBF_4 were purchased from Aldrich.

X-ray Structure Determination. Data collections were carried out on a Bruker SMART-CCD area diffractometer with graphite-monochromated Mo $K\alpha$ radiation ($\lambda = 0.71073 \text{ \AA}$) operating at 50 kV and 30 mA. A total of 1271 frames of intensity data were collected over a hemisphere of the reciprocal space by combination of three exposure sets. Each frame covered 0.3° in ω , and the first 50 frames were re-collected at the end of data collection to monitor crystal decay. Absorption corrections were applied using the SADABS program.³⁹ The structures were solved using the Bruker SHELXTL-PC software⁴⁰ by direct methods and refined by full-matrix least-squares methods on F^2 . Hydrogen atoms were included in calculated positions and refined in the riding mode, except those bonded to nitrogen atoms, which were located on residual density maps, then their positions fixed and refined in the riding mode. All non-hydrogen atoms were refined anisotropically. The details of the data collection and refinement are summarized in Table 2.

Preparation of $[\text{RuCl}_2(p\text{-cymene})(\kappa^1\text{-P-dpim})]$ (1a**).** dpim (518.4 mg, 1.95 mmol) was added over a solution of $[\text{RuCl}_2(p\text{-cymene})]_2$ (600 mg, 0.97 mmol) prepared in 120 mL of dichloromethane. The resulting solution was stirred for 15 h at rt. The solution was evaporated to dryness, and the resulting residue was washed with hexane ($3 \times 15 \text{ mL}$). An orange solid was obtained and dried under vacuum. Yield: 1.00 g (1.75 mmol, 89.4%). The compound was crystallized from $\text{CH}_2\text{Cl}_2/\text{hexane}$, obtaining crystals of **1a**· $1/2\text{CH}_2\text{Cl}_2$ suitable for an X-ray determination. Anal. Calcd for $\text{C}_{26.5}\text{H}_{30}\text{Cl}_3\text{N}_2\text{PRu}$ (614.91): C, 51.76; H, 4.92; N, 4.56. Found: C, 51.63; H, 4.81; N, 4.49. IR (Nujol, cm^{-1}): 348, 288 $\nu(\text{RuCl})$. ^1H NMR (chloroform-*d*): 8.22 (m, 4H, *ortho*-Ph); 7.33 (m, 7H, *m*, *para*-Ph and $\text{H}^4\text{-Im}$); 6.95 (t, 1H, $\text{H}^5\text{-Im}$); 5.391 (dd, $J_{\text{HH}} = 6.3$, $J_{\text{PH}} = 1.7$, 2H, $\text{CH}^{2,6}\text{-cym}$); 5.22 (d, $J_{\text{HH}} = 6.3$, 2H, $\text{CH}^{3,5}\text{-cym}$); 3.16 (s, 3H, *Me*-Im); 2.50 (spt, $J_{\text{HH}} = 7.0$, 1H, CHMe_2); 1.57 (s, 3H, *Me*-cym); 0.92 (d, $J_{\text{HH}} = 7.6$, 6H, CHMe_2) ppm. ^{13}C NMR (chloroform-*d*): 134.73 (d, $J_{\text{PC}} = 10$, 4C, *ortho*-Ph); 133.07 (d, $J_{\text{PC}} = 46.3$, 2C, *ipso*-Ph); 130.21 (d, $J_{\text{PC}} = 2.6$, 2C, *para*-Ph); 128.95 (d, $J_{\text{PC}} = 11.2$, 1C, $\text{C}^2\text{-Im}$); 127.81 (d, $J_{\text{PC}} = 10.3$, 4C, *meta*-Ph); 125.33 (d, $J_{\text{PC}} = 1.4$, 2C, *p*-Ph); 125.36 (s, 1C, CH-Im); 125.29 (s, 1C, CH-Im); 110.34 (s, 1C, $\text{C}^1\text{-Pr}$); 94.85 (s, 1C, C-Me cym); 92.11 (d, $J_{\text{PC}} = 4.3$, 2C, CH cym); 85.5 (d, $J_{\text{PC}} = 6.3$, 2C, CH cym); 36.07 (s, 1C, *Me*-Im); 29.98 (s, 1C, CHMe_2); 21.46 (s, 2C, CHMe_2); 16.8 (s, 1C, *Me*-cym) ppm. ^{31}P NMR (chloroform-*d*): 7.58 (s) ppm. FAB mass (m/z): 537 ($[\text{M} - \text{Cl}]^+$); 403 ($[\text{M} - \text{Cl} - \text{C}_{10}\text{H}_{14}]^+$). $\text{C}_{10}\text{H}_{14} = p\text{-cymene}$.

Preparation of $[\text{RuCl}_2(\text{C}_6\text{H}_6)(\kappa^1\text{-P-dpim})]$ (1b**).** dpim (351.5 mg, 1.32 mmol) was added over a suspension of $[\text{RuCl}_2(\text{C}_6\text{H}_6)(\text{CH}_3\text{CN})]$ (366 mg, 1.26 mmol) in 30 mL of acetonitrile. The mixture was stirred for 3 h at rt, and an orange-brown precipitate was formed. It was filtered and dried under vacuum. Yield: 585 mg (1.13 mmol, 90%). Crystallization from $\text{CH}_2\text{Cl}_2/\text{hexane}$ yielded crystals of **1b**· $2\text{CH}_2\text{Cl}_2$ suitable for an X-ray determination. Anal. Calcd for $\text{C}_{24}\text{H}_{25}\text{Cl}_6\text{N}_2\text{PRu}$ (686.20): C, 42.01; H, 3.67; N, 4.08. Found: C, 41.88; H, 3.75; N, 4.00. IR (Nujol, cm^{-1}): 297, 274 $\nu(\text{RuCl})$. ^1H NMR (chloro-

(38) (a) Bennett, M. A.; Huang, T. N.; Matheson, T. W.; Smith, A. K. *Inorg. Synth.* **1982**, *21*, 74. (b) Bennett, M. A.; Smith, A. K. *J. Chem. Soc., Dalton Trans.* **1974**, 233.

(39) Sheldrick, G. M. *SADABS. A Program for Empirical Absorption Correction of Area Detector Data*; University of Göttingen: Germany, 1996. Based on the method of Robert Blessing: Blessing, R. H. *Acta Crystallogr.* **1995**, *A51*, 33.

(40) Sheldrick, G. M. *SHELXS-97, A Program for Solving Crystal Structures and Crystal Structure Refinement*; University of Göttingen: Germany, 1997.

form-*d*): 8.03 (m, 4H, *ortho*-Ph); 7.37 (m, 6H, *meta*, *para*-Ph); 7.01 (s, 1H, *CH*-Im); 5.51 (d, $J_{\text{PH}} = 0.8$, 6H, C_6H_6); 3.2 (s, 3H, *N*-Me) ppm. ^{13}C NMR (chloroform-*d*): 134.38 (d, $J_{\text{CP}} = 10.1$, 4C, *ortho*-Ph); 131.34 (d, $J_{\text{CP}} = 48.3$, 2C, *ipso*-Ph); 130.78 (d, $J_{\text{CP}} = 2.7$, 2C, *para*-Ph); 129.65 (d, $J_{\text{CP}} = 12.7$, 1C, C^2 -Im); 128.11 (d, $J_{\text{CP}} = 10.6$, 4C, *meta*-Ph); 125.86 (s, 1C, *CH*-Im); 125.84 (s, 1C, *CH*-Im); 89.26 (d, $J_{\text{PC}} = 3.6$, 6C, C_6H_6); 36.08 (s, 1C, *N*-Me) ppm. ^{31}P NMR (chloroform-*d*): 11.85 (s) ppm. FAB MS (m/z): 481 ([M - Cl] $^+$); 403 ([M - Cl - C_6H_6] $^+$).

Preparation of [RuCl(*p*-cymene)(κ^2 -*PN*-dpim)]BF₄ (2a). TlBF₄ (66 mg, 0.23 mmol) was added to a solution of **1a** (130 mg, 0.23 mmol) in 10 mL of dichloromethane. A white precipitate was instantaneously formed. The mixture was stirred for 3 h. An orange solution was obtained after filtration. This was evaporated to dryness. The resulting orange powder was washed with pentane (3 × 10 mL). Yield: 0.126 g (0.2 mmol, 87.6%). Anal. Calcd for C₂₆H₂₉BClF₄N₂PRu (623.6): C, 50.06; H, 4.67; N, 4.49. Found: C, 49.9; H, 4.68; N, 4.59. IR (KBr, cm⁻¹): 1058 $\nu_{\text{a}}(\text{BF}_4^-)$; 547 $\delta_{\text{a}}(\text{BF}_4^-)$; Nujol: 399 $\nu(\text{RuCl})$. ^1H NMR (chloroform-*d*): 7.88 (m, 2H, *ortho*-Ph); 7.63 (m, 2H, *meta*-Ph); 1H, *para*-Ph); 7.59 (m, 1H, *para*-Ph); 7.49 (m, 2H, *ortho*-Ph); 1H, CH^4 -Im); 7.35 (m, 2H, *meta*-Ph); 1H, CH^5 -Im); 5.78 (d, $J_{\text{HH}} = 6.1$, 1H, CH^6 -cym); 5.65 (d, $J_{\text{HH}} = 6.1$, 1H, CH^5 -cym); 5.58 (d, $J_{\text{HH}} = 5.8$, 1H, CH^3 -cym); 5.10 (d, $J_{\text{HH}} = 5.8$, 1H, CH^2 -cym); 3.66 (s, 3H, *Me*-Im); 2.62 (spt, $^3J_{\text{HH}} = 6.9$, 1H, CHMe_2 -cym); 2.04 (s, 3H, *Me*-cym); 1.22 (d, $^3J_{\text{HH}} = 6.9$, 3H, CHMe_2 -cym); 1.17 (d, $^3J_{\text{HH}} = 6.9$, 3H, CMe_2 -cym) ppm. ^{13}C NMR (chloroform-*d*): 145.9 (d, $^1J_{\text{PC}} = 52.6$, 1C, C^2 -Im); 135.3 (d, $^2J_{\text{PC}} = 11.5$, 2C, *ortho*-Ph); 133.5 (d, $^4J_{\text{PC}} = 2.8$, 1C, *para*-Ph); 133 (d, $^4J_{\text{PC}} = 2.6$, 1C, *para*-Ph); 131.3 (d, $^3J_{\text{PC}} = 11.5$, 2C, *meta*-Ph); 131.1 (d, $^3J_{\text{PC}} = 14.6$, 1C, CH^4 -Im); 130.8 (d, $^3J_{\text{PC}} = 11.5$, 2C, *meta*-Ph); 129.6 (d, $^2J_{\text{PC}} = 11.4$, 2C, *ortho*-Ph); 129.2 (s, 1C, CH^5 -Im); 128.3 (d, $^1J_{\text{PC}} = 52.3$, 1C, *ipso*-Ph); 121.7 (d, $^1J_{\text{PC}} = 43.8$, 1C, *ipso*-Ph); 107 (d, $J_{\text{PC}} = 2.2$, 1C, CH^4 -cym); 100.8 (d, $J_{\text{PC}} = 1.5$, 1C, *CMe*-cym); 89.7 (d, $J_{\text{PC}} = 3.6$, 1C, CH^5 -cym); 85.6 (d, $J_{\text{PC}} = 5.6$, 1C, CH^6 -cym); 85.3 (d, $J_{\text{PC}} = 2.4$, 1C, CH^2 -cym); 84.04 (d, $J_{\text{PC}} = 2.7$, 1C, CH^3 -cym); 35.2 (s, 1C, *Me*-Im); 31.3 (s, 1C, CHMe_2 -cym); 23.3 (s, 1C, CHMe_2 -cym); 22.2 (s, 1C, CHMe_2 -cym); 19.1 (s, 1C, *CMe*-cym) ppm. ^{31}P NMR (chloroform-*d*): -13.27 (s) ppm. FAB MS (m/z): 537 ([M - BF₄] $^+$); 403 ([M - BF₄ - C₁₀H₁₄] $^+$). C₁₀H₁₄ = *p*-cymene.

Preparation of [RuCl(C₆H₆)(κ^2 -*PN*-dpim)]BF₄ (2b). TlBF₄ (45 mg, 0.16 mmol) was added over a solution of **1b** in dichloromethane (20 mL). After 20 min of stirring the solution become cloudy. The solution was stirred for 14 h. The white precipitate was filtrated, and the resulting pale orange solution was evaporated to dryness. The resulting solid was washed with pentane (3 × 10 mL) and dried under vacuum. Yield: 0.073 g (0.13 mmol, 83%). Anal. Calcd for C₂₂H₂₁BClF₄N₂PRu (567.51): C, 46.55; H, 3.73; N, 4.94. Found: C, 46.6; H, 3.51; N, 5.31. IR (KBr, cm⁻¹): 1058 $\nu_{\text{a}}(\text{BF}_4^-)$, 547 $\delta_{\text{a}}(\text{BF}_4^-)$. ^1H NMR (chloroform-*d*): 7.85 (m, 2H, *ortho*-Ph); 7.6 (m; 4H, *meta*-Ph); 1H, *CH*-Im); 7.51 (m, 2H, *ortho*-Ph); 7.32 (m; 2H, *para*-Ph); 1H *CH*-Im); 5.77 (d, $J_{\text{PH}} = 1.01$, 6H, C_6H_6); 3.63 (s, 3H, *Me*-Im) ppm. ^{13}C NMR (Chloroform-*d*): 138.0–127.0 (m, 15C, Ph, CH and C^2 -Im); 87.1 (d, $J_{\text{PC}} = 3.17$, 6C, C_6H_6); 35.12 (s, 1C, *Me*-Im) ppm. ^{31}P NMR (chloroform-*d*): -6.03 (s) ppm. FAB MS (m/z): 481 ([M - BF₄] $^+$); 446 ([M - BF₄ - Cl] $^+$); 403 ([M - BF₄ - C₆H₆] $^+$).

Preparation of [RuCl(*p*-cymene)(κ^1 -*N*-MeIm)(κ^1 -*P*-P(O₂Me)₂)Ph₂)]X; X = BF₄ (3a), BPh₄ (3d). Over a solution of **1a** (130 mg, 0.23 mmol) in 10 mL of dichloromethane another solution of NaBF₄ (24.9 mg, 0.23 mmol) in 10 mL of methanol was added. The mixture was stirred for 21 h. The solution was evaporated to dryness, and the residue was extracted with dichloromethane (5 mL). The resulting solution was filtered and evaporated to dryness. The resulting oil was triturated with pentane (15 mL). **3a** was obtained as a yellow solid after filtration. Yield: 0.149 g (0.168 mmol, 73%). An identical procedure was followed for **3d** using the corresponding amount of NaBPh₄ as precipitating salt.

3a: Anal. Calcd for C₂₇H₃₃BClF₄N₂OPRu (655.56): C, 49.47; H, 5.07; N, 4.27. Found: C, 49.05; H, 5.14; N, 4.62. IR (KBr): 1058 $\nu_{\text{a}}(\text{BF}_4^-)$; 547 $\delta_{\text{a}}(\text{BF}_4^-)$; Nujol: 399 $\nu(\text{RuCl})$. ^1H NMR (chloroform-*d*): 7.81 (s, 1H, CH^2 -Im); 7.61 (m, 2H, *ortho*-Ph); 7.49 (m, 1H, *para*-Ph); 7.44 (m, 2H, *ortho*-Ph); 7.31 (m, 1H, *para*-Ph); 7.23 (m, 2H, *meta*-Ph); 7.15 (m, 2H, *meta*-Ph); 7.10 (t, $^3J_{\text{HH}} \approx ^4J_{\text{HH}} = 1.4$, 1H, CH^5 -Im); 6.57 (t, $^3J_{\text{HH}} \approx ^4J_{\text{HH}} = 1.5$, 1H, CH^4 -Im); 5.77 (dd, $^3J_{\text{HH}} = 6.2$, $J_{\text{PH}} = 1.4$ 1H, *CH*-cym); 5.66 (d, $J_{\text{HH}} = 6.3$, 1H, *CH*-cym); 5.59 (dd, $^3J_{\text{HH}} = 6.1$, $J_{\text{PH}} = 1.4$, 1H, *CH*-cym); 5.49 (d, $J_{\text{HH}} = 6.1$, 1H, *CH*-cym); 3.63 (d, $^3J_{\text{PH}} = 11.3$, 3H, *POMe*); 3.6 (s, 3H, *Me*-Im); 2.5 (spt, $J_{\text{HH}} = 6.9$, 1H, CHMe_2 -cym); 2.12 (s, 3H, *CMe*-cym); 1.13 (d, $J_{\text{HH}} = 6.9$, 3H, CHMe_2); 1.12 (d, $J_{\text{HH}} = 6.9$, 3H, CHMe_2) ppm. ^{13}C NMR (chloroform-*d*): 143.26 (d, $^3J_{\text{CP}} = 1.8$, 1C, CH^2 -Im); 133.35 (d, $^2J_{\text{PC}} = 11.1$, 2C, *ortho*-Ph); 132.12 (d, $^4J_{\text{PC}} = 2.2$, 1C, *para*-Ph); 132.1 (d, $^1J_{\text{PC}} = 52.3$, 1C, *ipso*-Ph); 131.86 (d, $^2J_{\text{PC}} = 9.9$, 2C, *ortho*-Ph); 131.13 (d, $^4J_{\text{PC}} = 2.3$, 1C, *para*-Ph); 131.05 (s, 1C, CH^4 -Im); 130.47 (d, $^1J_{\text{PC}} = 46.5$, 1C, *ipso*-Ph); 128.54 (d, $^3J_{\text{PC}} = 10.4$, 2C, *meta*-Ph); 128.12 (d, $^3J_{\text{PC}} = 10$, 2C, *meta*-Ph); 121.24 (s, 1C, CH^5 -Im); 116.75 (d, $J_{\text{PC}} = 7.3$, 1C, *C*^{*Pr*}-cym); 103.88 (s, 1C, *CMe*-cym); 90.65 (d, $J_{\text{PC}} = 4.12$, 1C, CH^5 -cym); 89.86 (d, $J_{\text{PC}} = 4.22$, 1C, CH^3 -cym); 88.9 (d, $J_{\text{PC}} = 2.4$, 1C, CH^2 -cym); 87.2 (s, 1C, CH^6 -cym); 56.79 (d, $^2J_{\text{PC}} = 13$, 1C, *POMe*); 34.93 (s, 1C, *Me*-Im); 31.01 (s, 1C, CHMe_2 -cym); 22.23 (s, 1C, CHMe_2 -cym); 22.11 (s, 1C, CHMe_2 -cym); 18.76 (s, 1C, *CMe*-cym) ppm. ^{31}P NMR (chloroform-*d*): 129.7 (s) ppm. FAB MS (m/z): 569 ([M - BF₄] $^+$, 30%); 537 ([M - BF₄ - MeOH] $^+$, 15%); 487 ([M - BF₄ - MeImH] $^+$, 100%); 451 ([M - BF₄ - MeImH - HCl] $^+$, 55%); 421 ([M - BF₄ - MeImH - Cl - MeO] $^+$, 55%).

3d: Anal. Calcd for C₅₁H₅₃BClN₂OPRu (888.31): C, 68.96; H, 6.01; N, 3.15. Found: C, 68.51; H, 6.01; N, 3.43. IR (KBr, cm⁻¹): 2982, 2964, 1479, 1385, 743, 704, $\nu(\text{BPh}_4^-)$; Nujol: 409 $\nu(\text{RuCl})$. ^1H NMR (chloroform-*d*): 7.60–6.85 (m, 30H, (2 + 4)-Ph); 7.28 (s, 1H, CH^2 -Im); 6.52 (t, $^3J_{\text{HH}} \approx ^4J_{\text{HH}} = 1.5$, 1H, CH^5 -Im); 6.28 (t, $^3J_{\text{HH}} \approx ^4J_{\text{HH}} = 1.5$, 1H, CH^4 -Im); 5.28 (dd, $^3J_{\text{HH}} = 6.1$, $J_{\text{PH}} = 1.2$ 1H, *CH*-cym); 5.24 (d, $J_{\text{HH}} = 6.1$, 1H, *CH*-cym); 5.14 (dd, $^3J_{\text{HH}} = 6.1$, $J_{\text{PH}} = 1.3$, 1H, *CH*-cym); 4.93 (d, $J_{\text{HH}} = 6.1$, 1H, *CH*-cym); 3.45 (d, $^4J_{\text{PH}} = 11.1$, 3H, *MeO*); 3.08 (s, 3H, *Me*-Im); 2.52 (spt, $J_{\text{HH}} = 6.9$, 1H, CHMe_2 -cym); 1.89 (s, 3H, *CMe*-cym); 1.11 (d, $J_{\text{HH}} = 6.9$, 3H, CHMe_2); 1.10 (d, $J_{\text{HH}} = 6.9$, 3H, CHMe_2) ppm. ^{13}C NMR (chloroform-*d*): 164.35 (q, $J_{\text{CB}} = 49.3$, 4C, *ipso*-Ph-BPh₄); 140.74 (d, $^3J_{\text{CP}} = 1.8$, 1C, CH^2 -Im); 136.52 (q, $J_{\text{CB}} = 1.5$, 4C, *ortho*-Ph-BPh₄); 132.83 (d, $^4J_{\text{PC}} = 1.7$, 1C, CH^4 -Im); 132.76 (d, $^1J_{\text{PC}} = 48.1$, 1C, *ipso*-Ph); 132.69 (d, $^2J_{\text{PC}} = 10.9$, 2C, *ortho*-Ph); 132.36 (d, $^4J_{\text{PC}} = 2.2$, 1C, *para*-Ph); 131.86 (d, $^2J_{\text{PC}} = 9.9$, 2C, *ortho*-Ph); 131.46 (d, $^4J_{\text{PC}} = 2.8$, 1C, *para*-Ph); 129.72 (d, $^1J_{\text{PC}} = 46.5$, 1C, *ipso*-Ph); 128.87 (d, $^3J_{\text{PC}} = 10.4$, 2C, *meta*-Ph); 128.07 (d, $^3J_{\text{PC}} = 10.1$, 2C, *meta*-Ph); 125.82 (q, $J_{\text{CB}} = 2.7$, 4C, *meta*-Ph-BPh₄); 122.45 (s, 1C, CH^5 -Im); 122.03 (s, 4C, *para*-Ph-BPh₄); 116.64 (d, $J_{\text{PC}} = 5.4$, 1C, C^4 -cym); 102.43 (d, $J_{\text{PC}} = 1.5$, 1C, *CMe*-cym); 89.59 (d, $J_{\text{PC}} = 1.4$, 1C, CH^2 -cym); 89.5 (d, $J_{\text{PC}} = 2.5$, 1C, CH^6 -cym); 88.87 (d, $J_{\text{PC}} = 6.1$, 1C, CH^3 -cym); 87.74 (d, $J_{\text{PC}} = 2.8$, 1C, CH^5 -cym); 56.92 (d, $^3J_{\text{PC}} = 13.4$, 1C, *P*-*OMe*); 34.78 (s, 1C, *Me*-Im); 31.00 (s, 1C, CHMe_2 -cym); 22.23 (s, 1C, CHMe_2 -cym); 22.06 (s, 1C, CHMe_2 -cym); 18.63 (s, 1C, *CMe*-cym) ppm. ^{31}P NMR (chloroform-*d*): 128.84 (s) ppm. FAB mass (m/z): 569 ([M - BPh₄] $^+$); 487 ([M - BPh₄ - MeImH] $^+$); 452 ([M - BPh₄ - MeImH - HCl] $^+$); 421 ([M - BPh₄ - MeImH - Cl - MeO] $^+$).

Preparation of [RuCl(C₆H₆)(κ^1 -*N*-MeIm)(κ^1 -*P*-P(O₂Me)₂)Ph₂)]BF₄ (3b). Over a solution of **1b** (123 mg, 0.24 mmol) in 10 mL of dichloromethane another solution of NaBF₄ (26.7 mg, 0.24 mmol) in 10 mL of methanol was added. The mixture was stirred for 22 h. The solution was evaporated to dryness, and the residue was extracted with dichloromethane (5 mL). The resulting solution was filtered and evaporated to dryness. The resulting oil was triturated with pentane (15 mL). **3b** was obtained as a yellow solid after filtration. Yield: 0.122 g (0.204 mmol, 85%). Anal. Calcd for C₂₃H₂₅BClF₄N₂OPRu (599.5): C, 46.04; H, 4.17; N, 4.67. Found: C, 46.25; H, 4.09; N, 4.74. IR

(KBr, cm^{-1}): 1055 $\nu_{\text{d}}(\text{BF}_4^-)$; 541 $\delta_{\text{d}}(\text{BF}_4^-)$; Nujol: 294 $\nu(\text{Ru}-\text{Cl})$. ^1H NMR (chloroform-*d*): 7.78 (s, 1H, $\text{CH}^2\text{-Im}$); 7.6–7.2 (m, 10H, 2Ph); 7.15 (t, $^3J_{\text{HH}} \approx ^4J_{\text{HH}} = 1.5$, 1H, $\text{CH}^5\text{-Im}$); 6.6 (t, $^3J_{\text{HH}} \approx ^4J_{\text{HH}} = 1.5$, 1H, $\text{CH}^4\text{-Im}$); 5.9 (s, 6H, C_6H_6); 3.57 (d, $^4J_{\text{PH}} = 12$, 3H, MeO); 3.57 (s, 3H, Me-Im) ppm. ^{13}C NMR (chloroform-*d*): 143.1 (s, 1C, $\text{CH}^2\text{-Im}$); 132.82 (d, $^1J_{\text{PC}} = 51.2$, 1C, *ipso*-Ph); 132.77 (d, $^2J_{\text{PC}} = 11.1$, 2C, *ortho*-Ph); 132.27 (d, $^4J_{\text{PC}} = 2.3$, 1C, *para*-Ph); 131.85 (d, $^2J_{\text{PC}} = 10.4$, 2C, *ortho*-Ph); 131.51 (s, 1C, $\text{CH}^4\text{-Im}$); 131.49 (d, $^4J_{\text{PC}} = 2.2$, 1C, *para*-Ph); 130.25 (d, $^1J_{\text{PC}} = 48.4$, 1C, *ipso*-Ph); 128.78 (d, $^3J_{\text{PC}} = 10.5$, 2C, *meta*-Ph); 128.34 (d, $^3J_{\text{PC}} = 10.5$, 2C, *meta*-Ph); 121.31 (s, 1C, $\text{CH}^5\text{-Im}$); 91.09 (d, $J_{\text{PC}} = 3.4$, 6C, C_6H_6); 56.6 (d, $^3J_{\text{PC}} = 11.4$, 1C, OMe); 34.92 (s, 1C, Me-Im). ^{31}P NMR (chloroform-*d*): 130.27 (s) ppm. FAB mass (*m/z*): 513 ($[\text{M} - \text{BF}_4]^{+}$, 55%); 431 ($[\text{M} - \text{BF}_4 - \text{MeImH}]^{+}$, 100%); 395 ($[\text{M} - \text{BF}_4 - \text{MeImH} - \text{HCl}]^{+}$, 80%), 365 ($[\text{M} - \text{BF}_4 - \text{MeImH} - \text{MeO} - \text{Cl}]^{+}$, 100%).

Preparation of $[\text{RuCl}_2(p\text{-cymene})(\kappa^1\text{-P-dpimH})\text{BF}_4$ (**4a**).

Over a solution of **1a** (0.080 g, 0.14 mmol) in acetone (30 mL) a solution of HBF_4 (19.3 μL of a solution 54% w/w, 0.14 mmol) in diethyl ether was added. The solution was stirred for 15 min, and the solution was evaporated to dryness. The resulting oil was washed with pentane (15 mL), giving a red solid of **4a**. Yield: 0.085 g (0.13 mmol, 92%). Crystals of **4a**- CH_2Cl_2 suitable for an X-ray determination were obtained from CH_2Cl_2 /hexane. Anal. Calcd for $\text{C}_{27}\text{H}_{22}\text{BCl}_4\text{F}_4\text{N}_2\text{PRu}$ (745.20): C, 43.52; H, 4.33; N, 3.76. Found: C, 43.65; H, 4.25; N, 3.85. IR (KBr, cm^{-1}): 1058 $\nu_{\text{d}}(\text{BF}_4^-)$; 535 $\delta_{\text{d}}(\text{BF}_4^-)$; Nujol: 348, 293 $\nu(\text{Ru}-\text{Cl})$. ^1H NMR (chloroform-*d*): 13.1 (bs, 1H, NH); 7.94 (m, 4 H, *ortho*-Ph); 7.64 (m, 6H, *meta* and *para*-Ph); 7.6 (s, 1H, $\text{CH}^4\text{-Im}$); 7.38 (s, 1H, $\text{CH}^5\text{-Im}$); 5.46 (d, $J_{\text{HH}} = 5.6$, 2H, CH-cym); 5.38 (d, $J_{\text{HH}} = 5.6$, 2H, CH-cym); 3.26 (s, 3H, Me-Im); 2.54 (spt, $^3J_{\text{HH}} = 6.9$, 1H, $\text{CHMe}_2\text{-cym}$); 1.75 (s, 3H, CMe-cym); 0.85 (d, $^3J_{\text{HH}} = 6.9$, 6H, $\text{CHMe}_2\text{-cym}$) ppm. ^{13}C NMR (acetone-*d*₆): 138 (d, $^1J_{\text{PC}} = 65.3$, 1C, $\text{C}^2\text{-Im}$); 134.3 (d, $^1J_{\text{PC}} = 21.8$, 2C, *ipso*-Ph); 133.1 (d, $^2J_{\text{PC}} = 10.7$, 4C, *ortho*-Ph); 133.1 (d, $^4J_{\text{PC}} = 2.4$, 2C, *para*-Ph); 130 (d, $^3J_{\text{PC}} = 10.7$, 4C, *meta*-Ph); 128.6 (s, 1C, $\text{CH}^4\text{-Im}$); 127.8 (s, 1C, $\text{CH}^5\text{-Im}$); 111.1 (s, 1C, $\text{C}^{\text{Pr}}\text{-cym}$); 97.2 (s, 1C, CMe-cym); 92.1 (d, $J_{\text{PC}} = 4.3$, 2C, $\text{CH}^{2,6}\text{-cym}$); 87.4 (d, $J_{\text{PC}} = 6.2$, 2C, $\text{CH}^{3,5}\text{-cym}$); 37.6 (s, 1C, Me-Im); 30.5 (s, 1C, $\text{CHMe}_2\text{-cym}$); 20.8 (s, 2C, $\text{CHMe}_2\text{-cym}$); 16.9 (s, 1C, CMe-cym) ppm. ^{31}P NMR (chloroform-*d*): 23.92 (s) ppm. FAB MS (*m/z*): 573 ($[\text{M} - \text{BF}_4]^{+}$); 537 ($[\text{M} - \text{BF}_4 - \text{H} - \text{Cl}]^{+}$); 403 ($[\text{M} - \text{BF}_4 - \text{H} - \text{Cl} - (\text{C}_{10}\text{H}_{14})^{+}]$). $\text{C}_{10}\text{H}_{14} = p\text{-cymene}$.

Preparation of $[\text{RuCl}_2(\text{C}_6\text{H}_6)(\kappa^1\text{-P-dpimH})\text{BF}_4$ (**4b**).

Over a suspension of **1b** (0.050 g, 0.09 mmol) in acetone (30 mL) a solution of HBF_4 (12.2 μL of a solution 54% w/w, 0.09 mmol) in diethyl ether was added. The solution was stirred for 15 min, and the solution was evaporated to dryness. The resulting oil was washed with pentane (15 mL), giving a red solid of **4b**. Yield: 0.052 g (0.086 mmol, 89%). Crystals of **4b** suitable for an X-ray determination were obtained from CH_2Cl_2 /hexane. Anal. Calcd for $\text{C}_{22}\text{H}_{22}\text{BCl}_2\text{F}_4\text{N}_2\text{PRu}$ (604.17): C, 43.74; H, 3.67; N, 4.64. Found: C, 43.59; H, 3.73; N, 4.73. IR (KBr, cm^{-1}): 1061 $\nu_{\text{d}}(\text{BF}_4^-)$; 538 $\delta_{\text{d}}(\text{BF}_4^-)$; Nujol: 358, 319 $\nu(\text{Ru}-\text{Cl})$. ^1H NMR (acetone-*d*₆): 13.04 (bs, 1H, NH); 8.08 (m, 4H, *ortho*-Ph); 7.89 (pst, 1H CH-Im); 7.73 (m, 7H, *meta*- and *para*-Ph); 1H, CH-Im); 5.84 (d, $J_{\text{PH}} = 0.9$, 6H, C_6H_6); 3.53 (s, 3H, Me-Im) ppm. ^{13}C NMR (acetone-*d*₆): 133.76 (d, $^2J_{\text{PC}} = 11.3$, 4C, *ortho*-Ph); 133.33 (d, $^4J_{\text{PC}} = 2.5$, 2C, *para*-Ph); 130.1 (d, $^3J_{\text{PC}} = 10.8$, 4C, *meta*-Ph); 128.53 (s, 1C, CH-Im); 128.46 (s, 1C, CH-Im); 127.86 (d, $^1J_{\text{PC}} = 50$, 2C, *ipso*-Ph); 121.4 (d, $^1J_{\text{PC}} = 2.8$, 1C, $\text{C}^2\text{-Im}$); 90.55 (d, $J_{\text{PC}} = 3.6$, 6C, C_6H_6); 37.94 (s, 1C, Me-Im) ppm. ^{31}P NMR (acetone-*d*₆): 35.1 (s) ppm. FAB MS (*m/z*): 517 ($[\text{M} - \text{BF}_4]^{+}$); 481 ($[\text{M} - \text{BF}_4 - \text{H} - \text{Cl}]^{+}$); 403 ($[\text{M} - \text{BF}_4 - \text{H} - \text{Cl} - (\text{C}_6\text{H}_6)]^{+}$).

Preparation of $[\text{RuCl}_2(p\text{-cymene})(\kappa^1\text{-P-PPh}_2\text{pyH})\text{BF}_4$ (4c**).** Over a suspension of **1c** (0.030 g, 0.05 mmol) in acetone (10 mL) a solution of HBF_4 (8 μL of a solution 54% w/w, 0.09 mmol) in diethyl ether was added. The solution was stirred for 20 min and evaporated to dryness. The resulting oil was triturated with diethyl ether (2 \times 10 mL), giving an orange

solid of **4c**. Yield: 0.030 g (0.045 mmol, 90%). Anal. Calcd for $\text{C}_{27}\text{H}_{29}\text{BCl}_2\text{F}_4\text{NPRu}$ (657.29): C, 49.34; H, 4.45; N, 2.13. Found: C, 49.09; H, 4.41; N, 2.18. IR (Nujol, cm^{-1}): 1051 $\nu_{\text{d}}(\text{BF}_4^-)$; 524 $\delta_{\text{d}}(\text{BF}_4^-)$; 328 $\nu(\text{RuCl})$. ^1H NMR (acetone-*d*₆): 9.15 (m, 1H, py); 8.68 (m, 1H, py); 8.27 (m, 1H, py); 8.11 (m, 1H, py); 7.94 (m, 4H, *ortho*-Ph); 7.72 (m, 6H, *meta*- and *para*-Ph); 5.79 (d, $J_{\text{HH}} = 6.4$, 2H, CH-cym); 5.62 (d, 2H, CH-cym); 2.61 (spt, $^3J_{\text{HH}} = 7.1$, 1H, $\text{CHMe}_2\text{-cym}$); 1.89 (s, 3H, CMe-cym); 1.12 (d, $^3J_{\text{HH}} = 6.9$, 6H, $\text{CHMe}_2\text{-cym}$) ppm. ^{13}C NMR (acetone-*d*₆): 135.09 (d, $^2J_{\text{PC}} = 10.5$, 4C, *ortho*-Ph); 128.74 (d, $^4J_{\text{PC}} = 2.5$, 2C, *para*-Ph); 130.32 (d, $^3J_{\text{PC}} = 10.0$, 4C, *meta*-Ph); 147.29 (d, $^1J_{\text{PC}} = 3.4$, py); 143.53 (d, $^1J_{\text{PC}} = 5.0$, py); 133.22 (py), 129.41 (py); 112.17 (d, $J_{\text{CP}} = 3.1$, 1C, $\text{C}^{\text{Pr}}\text{-cym}$); 100.01 (s, 1C, CMe-cym); 89.33 (d, $J_{\text{PC}} = 5.0$, 2C, $\text{CH}^{2,6}\text{-cym}$ or $\text{CH}^{3,5}\text{-cym}$); 89.94 (d, $J_{\text{PC}} = 5.0$, 2C, $\text{CH}^{2,6}\text{-cym}$ or $\text{CH}^{3,5}\text{-cym}$); 31.31 (s, 1C, $\text{CHMe}_2\text{-cym}$); 21.98 (s, 2C, $\text{CHMe}_2\text{-cym}$); 17.85 (s, 1C, CMe-cym) ppm. ^{31}P NMR (acetone-*d*₆): 21.98 (s) ppm.

Monitoring of the Transformation of **1a, **2a**, or **4a** in Methanol-*d*₄ with Time.** The reaction of **1a**, **2a**, or **4a** with methanol-*d*₄ at 25 $^{\circ}\text{C}$ to give **3a** or **3e** was monitored by ^1H NMR spectroscopy. The intensity of the *Me-Im* signals of each complex was taken into account to express graphically the evolution of the reactions and to calculate the different kinetic constants.

A sample of **1a** (4 mg, 0.007 mmol) was introduced into an NMR tube (5 mm). Air was evacuated, and 350 μL of methanol-*d*₄ and 100 μL of chloroform-*d* were introduced into the tube with a microsyringe (500 μL). The tube was sealed and a homogeneous solution was formed after shaking. The reaction was monitored by ^1H NMR spectroscopy during 12 h by introducing the tube into the probe, which had been previously equilibrated to 25 $^{\circ}\text{C}$. A similar procedure was used to follow the reaction of **2a** (4 mg, 0.006 mmol) with methanol-*d*₄ (350 μL of methanol-*d*₄ and 100 μL of chloroform-*d*) or from **4a** (4 mg, 0.006 mmol) and 450 mL of methanol-*d*₄.

Analogous reactions for **1a** and **2a** were monitored in the presence of LiCl. For instance, a sample of **2a** (4 mg, 0.006 mmol) and LiCl (1.6 mg, 0.038 mmol) were dissolved in an NMR tube with 1 mL of methanol-*d*₄ and 1 μL of chloroform-*d*. The reaction was monitored by ^1H NMR spectroscopy as outlined above.

Kinetic Measurements. The reaction of **1a** or **2a** with methanol was studied using a Shimadzu UV-160 spectrophotometer. The progress of the reaction was followed by measuring the optical absorbance of **1a** at 373 nm ($\epsilon = 2933 \text{ M}^{-1} \text{ cm}^{-1}$) or **2a** at 199 nm ($\epsilon = 1322 \text{ M}^{-1} \text{ cm}^{-1}$). All the kinetic runs were initiated by addition of methanol to a solution that contained the complex **1a** or **2a** in chloroform. The initial rates method was used for the kinetic analysis.

Hydrogen Transfer Catalysis with the Precatalysts **1a and **2a**.** In a typical procedure without base, the substrate, cyclohexanone (2 mL, 19.26 mmol), was added to a solution of the precatalyst **1a** (5.51 mg, 9.63×10^{-3} mmol) in 2-propanol (15 mL) (ketone:precatalyst = 2000:1) and the mixture was stirred at the reflux temperature.

In a typical procedure with base, the substrate, cyclohexanone (2 mL, 19.26 mmol), was added to a solution of the precatalyst **1a** (5.51 mg, 9.63×10^{-3} mmol) and KOH (177 mg, 3.2 mmol) in 2-propanol (15 mL) (ketone:precatalyst:KOH = 2000:1:333) and the mixture was stirred at the reflux temperature.

Hydrogenation with Molecular Hydrogen. The hydrogenation reactions were carried out in an autoclave with a pressure of 30 atm of H_2 in a thermostatic bath and with magnetic stirring. In a typical procedure, the substrate, phenylacetylene (1.1 mL, 10 mmol), was added to a solution of the precatalyst **2a** (6.2 mg, 1×10^{-2} mmol) in 2-propanol (15 mL) (substrate:precatalyst = 1000:1).

Conditions of the GC analysis: glass capillary column HP-PPFA (30 m \times 0.25 mm \times 0.25 μm). He as carrier gas. In the analysis of the hydrogenation of cyclohexanone, the column

was heated at 80 °C during 0.8 min and afterward heated at 12 °C/min to 110 °C. $t_R(\text{cyclohexanone}) = 2.142$ min, $t_R(\text{cyclohexanol}) = 2.947$ min. In the analysis of the hydrogenation of phenylacetylene, the column was heated at 60 °C during 1 min and afterward heated at 10 °C/min to 80 °C. $t_R(\text{phenylacetylene}) = 4.64$ min, $t_R(\text{styrene}) = 3.069$ min, $t_R(\text{ethylbenzene}) = 1.776$ min, 60 °C (1min) to 80 °C (3.5min) at 10 °C/min.

Acknowledgment. We are grateful to the Spanish DGES/MCyT (Project No. BQU-2002-00286) and Consejería de Ciencia y Tecnología of JCCLM (PBI-02-002)

for financial support. We also thank J. J. Delgado from SCAI, University of Burgos, Spain, for carrying out elemental analyses.

Supporting Information Available: Tables and CIF files of X-ray structural data, including data collection parameters, positional and thermal parameters, bond distances and angles for complexes, and additional structural views of complexes **1a**, **1b**, **4a**, and **4b**. This material is available free of charge via the Internet at <http://pubs.acs.org>.

OM049438O